

Seminar series no. 196

Vegetation indices, FAPAR and spatial seasonality analysis of crops in southern Sweden



RAUNAQ JAHAN

2010

Department of Earth and Ecosystem Sciences

Physical Geography and Ecosystems Analysis

Lund University

Sölvegatan 12



Raunaq Jahan 2010

Master degree thesis in Physical Geography and Ecosystem Analysis

Supervisor

Dr. Lars Eklundh

Department of Physical Geography and Ecosystem Analysis

Lund University

ACKNOWLEDGMENT

I would like to give a very special thanks to my supervisor Dr.Lars Eklundh for giving lots of inspiration and support during my work and never-ending encouragement when writing this report. He was always patient to discuss technical difficulties and providing valuable advises on the TIMESAT output and analysis. Thanks Margereta Hellström also for all assistance during the process data and finding helpful background material for development of my project.

Furthermore, I would like to thank Dr. Sharif Enamul Kabir for providing me a study leave and opportunity to finish my MS program in between my service period. A special thanks also to my class mates Rado, Hongxiao for their great assistance and advice to improve my report.

Last but not least, I would like to thank my husband Mahmudul Hasan to accompanying me during my study in Sweden and my daughter Raisa Hasan Progoty , who missed me during my study time at University.

Abstract

Remote sensing is an extensively used technique in ecosystem monitoring or analyzing the carbon balance on the earth surface. The most dominant part of south west Skåne is agricultural land and MODIS derived Vegetation Indexes (VIs) are able to investigate the seasonality of crop fields. The values of VIs represent the different stages of spring greening up of crops and it shows the non-linear and strong relationship with ground-measured fraction of absorbed photosynthetically active radiation (FAPAR). Crop productivity is related to absorbed radiation and there are some evident from previous studies which are able to provide relationship between VIs and Gross Primary Productivity (GPP). So, when the measured FAPAR describe more than 70% of NDVI (Normalized difference vegetation index) and WDRVI (Wide dynamic range vegetation index) of MODIS data, it is possible to monitor the productivity of crops through remote sensing tool. TIMESAT software was used to analyze graphical as well as image based vegetation indices and seasonality parameters. As there were two growing seasons in the study area, TIMESAT sometimes failed to cover the second season in seasonality analysis. Spatial analysis of crop phenology revealed dynamic for the area, and the phonological parameters varied according to VIs. Seasonality analysis for the four study area showed slight decreasing trend of the parameters in both indices, but image based spatial analysis was able to distinguish both increase and decrease of the parameters in different parts of south west Skåne. Spatial analysis of phenology requires more than one index results of an area to get less problematic results.

Keywords: Geography, Physical Geography, MODIS, FAPAR, NDVI, WDRVI, carbon uptake, TIMESAT, south west Skåne.

Table of contents

| | |
|---|-----|
| ACKNOWLEDGMENT | iii |
| Abstract..... | v |
| Table of contents..... | vi |
| 1. Introduction..... | 1 |
| 1.1 Importance of crops..... | 1 |
| 1.2 Aim of the Study..... | 2 |
| 2. Background..... | 3 |
| 2.1 Satellite remote sensing and MODIS | 3 |
| 2.2 Spectral characteristics of vegetation..... | 4 |
| 2.3 Vegetation Indices..... | 5 |
| 2.3 a) NDVI | 6 |
| 2.3 b) WDRVI | 6 |
| 2.4 Carbon Uptake | 7 |
| 3. Material and methods..... | 8 |
| 3.1 Study area | 8 |
| 3.2 Measurements of photosynthetic photon flux density | 11 |
| 3.2.a) TRAC reading from fields: | 11 |
| 3.2.b) Fraction of green portion in the site:..... | 12 |
| 3.3 Time series and statistical analysis | 13 |
| 4. Results | 15 |
| 4.1 FAPAR observation from field..... | 15 |
| 4.2 Extraction of MODIS NDVI and WDRVI through TIMESAT in ASCII format..... | 16 |
| 4.3 Relationship between FAPAR and MODIS NDVI | 23 |
| 4.4 Relationship between FAPAR and MODIS WDRVI | 24 |
| 4.5 Seasonality analysis from images..... | 25 |

| | |
|---|----|
| 4.5. a) Length of season | 25 |
| 4.5. b) Amplitude of season | 27 |
| 4.5.c) Small integral of season | 30 |
| 5. Discussion..... | 33 |
| 5.1. Discussion on project result | 33 |
| 5.2. Possible errors from project | 34 |
| 6. Conclusion | 36 |
| 6.1. Conclusion on project result | 36 |
| 6.2. Further studies | 36 |
| References..... | 38 |
| Appendix A..... | 41 |
| Publication list: | 42 |

1. Introduction

1.1 Importance of crops

The increasing trend of population demands the increase of crop production globally. According to Gitelson *et al.* (2008), crops are the most pervasive anthropogenic biome which is playing an important role in the global cycles of carbon, water and nutrients. The changing pattern of carbon is the present concern in the world as well as in Europe as global warming has the direct effect on the growing season of agriculture. Field management practices for increasing crop yields and decreasing forest or pasture have effect on the amount of atmospheric carbon fixed through photosynthesis and on the release of carbon due to organic matter decomposition (Gitelson *et al.* 2008).

Regional carbon budget can be assessed from remote sensing as vegetation productivity is directly related with the photosynthesis process, carbon uptake and interaction of solar radiation. Sensors are able to estimate vegetation indices (VIs)*, which represent different stages of spring green up of crops. There have been tremendous uses of VIs in forest or in peat land but very less study found on crops or managed vegetation cover. Southern Sweden is one of the prominence fertile agricultural part and crops play a vital roll in carbon sequestration of this region. Though the peak time for high carbon uptake is almost one-third of the whole growing season, but it should not be neglected in carbon balance of the region.

Satellite sensor data generally include noises and to analyze seasonality from those data, function fitting or simple filters are able to generate smooth time series (Jönsson & Eklundh, 2003). Like other vegetation cover crops have significant signature on its seasonality and clear annual growth and decline pattern which allows for the fitting of sinusoidal or bell-shaped functions in a time-series through TIMESAT software (Jönsson & Eklundh, 2003). The time series of NDVI (Normalized Difference Vegetation Index) and WDRVI (Wide dynamic range of vegetation index) generally cover the whole growing season and phenological parameters can be validated from real world data.

Spatial pattern of crop phenology was also an important part of this research and MODIS (Moderate Resolution Imaging Spectroradiometer) images were the only source of information on vegetation indices in spatial format. The seasonality pattern of south west Skåne is somehow

* All Abbreviations are sorted in Appendix A.

controlled by coastal climate, so it could be analyze as spatial pattern in case of phenology changes on crops.

1.2 Aim of the Study

The aims of this project were:

- I) to compare satellite derived vegetation indexes with the observed FAPAR or spring green up of barley and wheat fields in Lund kommun for a growing season.
- II) to analyze the seasonality pattern of crops in south west Skåne from satellite images.

2. Background

2.1 Satellite remote sensing and MODIS

According to Colwell (1960) remote sensing is the measurement of some property of an object or phenomenon, by a recording device that is not in physical or intimate contact with the object or phenomenon under study. Remote sensing is a tool or technique which uses sophisticated sensors to measure the amount of electromagnetic energy emitting an object or geographic area from a distance.

Sensors can obtain very specific information about an object or the geographic extent of a phenomenon through the electromagnetic energy emitted or reflected from an object (Jensen, 2000). When electromagnetic energy reaches to an object, it can be absorbed or reflected or transmitted through the object. The reflected energy from an object creates the specific signature over the electromagnetic spectrum. The spectral signature varies object to object by their physical or chemical properties (e.g. spectral signature varies according to content of water in leaves in specific band of sensor). Remote sensing technique can be operated by active (by own energy source) or passive ways and the most remote sensing is performed in passive way, as it uses the Sun's energy for illumination.

MODIS is an instrument aboard Terra and Aqua satellites by NASA. These satellites are placed in sun synchronous near-polar orbits with Terra passing over the equator from south to north at 10:30 a.m. and Aqua passing the equator in the other direction at 1:30 p.m. MODIS is able to provide daily observation of the entire surface of the Earth through its orbit (NASA 1, 2010). It has 36 bands and spatial resolution of 250 m (bands 1-2), 500 m (bands 3-7) and 1000 m (bands 8-36). In this study one MODIS data product from the Terra satellite was used, MOD09Q1 which contains atmospherically corrected surface reflectance from red and near infrared (NIR) bands at 250 m spatial resolutions. Table 1 shows the information on bandwidth of the bands used in this product.

Table 1: Selected MODIS spectral bands (<http://modis.gsfc.nasa.gov/about/specifications.php>)

| Primary use | Band | Bandwidth in nm | Spectral Radiance (W/m ² - μm -sr) | Required SNR(Signal – to- noise ratio) |
|----------------------------------|--------|-----------------|---|---|
| Land/ Cloud/ Aerosols Boundaries | 1(Red) | 620- 670 | 21.8 | 128 |
| | 2(NIR) | 841 - 876 | 24.7 | 201 |

Single grid cell subsets from the Terra/MODIS 8-day 250 m collection were downloaded from NASA website. There are 36 horizontal tiles and 18 vertical tiles in the Integerized Sinusoidal projection of MODIS product. In that projection it is possible to map 1km, 0.5km and 0.25km size of pixel resolution. The maps were produced from Tile coordinates. MODLAND tile calculator is able to calculate the specific tile for the study location with its latitude and longitude values (MODLAND, 2005).

2.2 Spectral characteristics of vegetation

Plants have distinct response to the solar radiation and chlorophyll in photosynthetic cells absorbs this radiation in the visible region of the solar spectrum (Larcher, 2003). Figure 1(i) shows the spectral reflectance characteristics of vegetation cover in different situations, where in NIR healthy green vegetation has higher reflectance than stressed and severely stressed vegetation. The amount of reflected radiation of healthy vegetation in near-infrared is remarkable which is shown in Figure 1(ii) and able to provide information about plant senescence (Jensen, 2000). Figure 1 (ii) and (iii) show the reflectance properties of photosynthesizing green Sweetgum leaf (*Liquidambar styraciflua* L.) in figure (iii) a, senescing yellow and red leaves in b-c and d is the brown leaf on the ground.

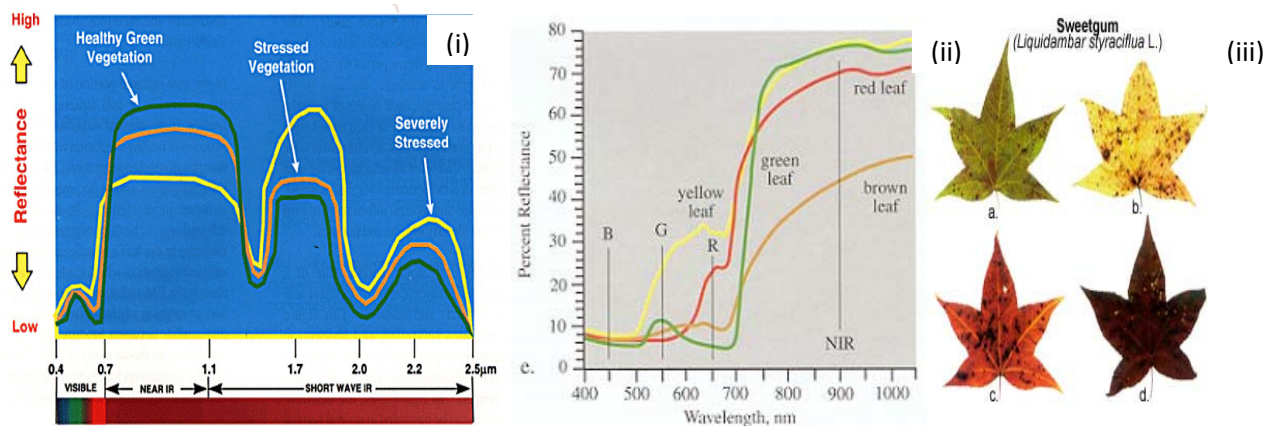


Figure 1: Spectral reflectance properties of vegetation in different situation.(Source: i-CSC and ii, iii - Jensen, 2000)

According to Jensen (2000) increasing ripeness of vegetation reflects more near-infrared energy while at the same time absorbing red radiant flux for photosynthetic purposes. Jensen described this situation by a soil line for a growing season of an agricultural pixel, where it is clearly visible that as the biomass increases, the field's location in the red and near-infrared spectral space

moves farther away from the soil line (Figure 2).

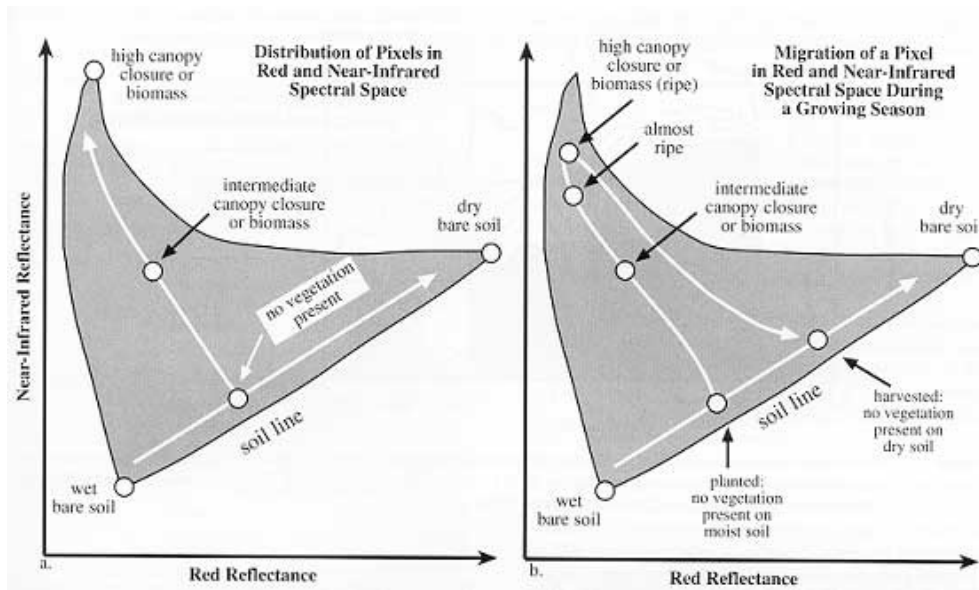


Figure 2: a) the gray shaded area is the distribution of all the pixels in a scene in red and near-infrared multispectral space. b) The migration of a single vegetated agricultural pixel in red and near-infrared multispectral space during a growing season (Source: Jensen, 2000).

2.3 Vegetation Indices

Vegetation indices (VIs) are dimensionless, radiometric measures which function as indicators of relative abundance and activity of green vegetation and include leaf area index (LAI), percentage green cover, chlorophyll content, green biomass, and absorbed photosynthetically active radiation (APAR) (Jensen, 2000; Glenn *et al.* 2008). These Indices were first developed in the 1970s and have been highly successful to assess different vegetation condition till now. According to Running *et al.*, (1994) and Huete and Justice (1999) a vegetation index should fulfill the following criteria:

- VI maximizes sensitivity to plant biophysical parameters. It response in a linear order that facilitate validation of the index.
- It normalizes or models external effects such as Sun angle, viewing angle and the atmosphere for consistent spatial and temporal comparisons.

- It normalizes internal effects such as canopy background variations, including topography, soil variations and differences in senesced or woody vegetation.
- Vegetation indexes can be proxies for other canopy attributes like LAI (Glenn *et al.*, 2008).

2.3 a) NDVI

Normalized difference vegetation index (NDVI) is widely adopted vegetation index which was established by Rouse *et al.* (1974). This index value is calculated with the two spectral bands: red(R) and near-infrared (NIR).

$$NDVI = \frac{NIR - R}{NIR + R} \quad (1)$$

NDVI was built on the observation that chlorophylls a and b in green leaves strongly absorb light in the red, with maximum absorption at about 690nm and the cell walls strongly scatter (reflect and transmit) light in the NIR region (about 850 nm)(Glenn *et al.*, 2008)

It is the mostly used indices among all indices. The range of the NDVI varies from -1 to 1, where negative values indicate water bodies, small positive values means little or no green vegetation and values nearer to 1 indicate dense vegetation. The value of NDVI is affected by soil background, optical properties and leaf angle distributions (Leeuwen & Huete, 1996).

2.3 b) WDRVI

As NDVI values saturates after 0.7, the greening trend and NDVI relation would lose its linear trend, so Gitelson (2004) introduced a weighting parameter α to the near infrared reflectance which works like tuning of NDVI value.

$$WDRVI = \frac{\alpha * NIR - R}{\alpha * NIR + R} \quad (2)$$

Here the value of $\alpha=1$ means $WDRVI = NDVI$, and $\alpha=R/NIR$, then $WDRVI= 0$. The value of α is generally <1 and varies between 0.02 and 0.5. The range of WDRVI is -0.6 to 0.6. Gitelson (2004) also tested different levels of α (0.20, 0.10, 0.05) for a specific image and Henebry *et al.* (2004) got $\alpha=0.20$ was the best suited value. This value ($\alpha=0.20$) was shown more effective for proximal sensors (Gitelson, 2004), Advanced Very High Resolution Radiometer (AVHRR) (Viña *et al.* 2004) and Landsat ETM + (Henebry *et al.* 2004) imagery in the absence of atmospheric correction, so the same coefficient value for agricultural sites was used for this project to explore the potential of the WDRVI in revealing more variation in high LAI.

2.4 Carbon Uptake

Monteith (1972) suggested the linear correlation between GPP of crops and the amount of absorbed photosynthetically active radiation,

$$\text{GPP} = \varepsilon \times \sum (\text{FAPAR} \times \text{PAR}) \quad (3)$$

where PAR is the incident photosynthetically active radiation, FAPAR is the fraction of PAR absorbed by the crop canopy and ε is light use efficiency. This model can be applied with the vegetation indices (VI), acquired by operational satellite with fine or coarse resolution data.

Gitelson *et al.* (2008) made the relationship between daytime GPP in crop with some vegetation indices using Landsat data, where they established the correlation between NDVI and GPP as well as WDRVI and GPP. The correlation was 95% for NDVI and 96% for WDRVI. They found asymptotic relationship between NDVI and GPP and also for WDRVI and GPP, with a significant decrease in the slope when GPP exceeds 10 $\text{gC.m}^{-2}.\text{d}^{-1}$ for NDVI and 15 $\text{gC.m}^{-2}.\text{d}^{-1}$ for WDRVI. It was a limitation of NDVI that it was unable to give accurate estimation at moderate to high vegetation densities and of $\text{GPP} > 10 \text{ gC.m}^{-2}.\text{d}^{-1}$ which corresponds to more than two months of the growing season.

They also analyzed the noise equivalent of GPP (NE ΔGPP) estimation for NDVI and WDRVI where they tried to show NDVI had minimal NE ΔGPP for $\text{GPP} < 5 \text{ gC.m}^{-2}.\text{d}^{-1}$ at $\text{GPP} > 8 \text{ gC.m}^{-2}.\text{d}^{-1}$ the NE ΔGPP increased exponentially and reached 28 $\text{gC.m}^{-2}.\text{d}^{-1}$ for $\text{GPP} = 23 \text{ gC.m}^{-2}.\text{d}^{-1}$. Figure 3 shows WDRVI had the lowest noise equivalent in the range of GPP from 5 to 12 $\text{gC.m}^{-2}.\text{d}^{-1}$ and it started to increase beyond 10 $\text{gC.m}^{-2}.\text{d}^{-1}$ but lower rate than that of NDVI. It means that WDRVI has lower noises than NDVI estimating the carbon uptake of crops.

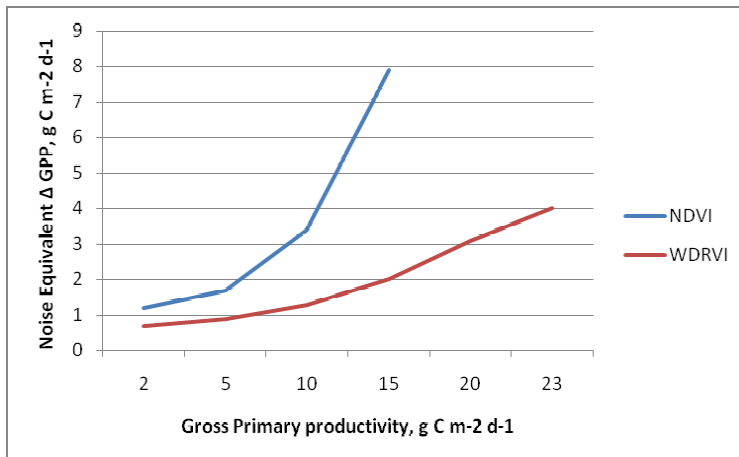


Figure 3: Noise equivalent of GPP estimation by two VIs plotted versus daytime GPP (Source: After Gitelson *et al.*, 2008).

3. Material and methods

3.1 Study area

The crop fields of the project were chosen in the south western part of Skåne (Scania), beside Lund's Kommun in Sweden. The annual average temperature of Scania is about +7°C (Bärring *et al.*, 2003). The average temperature in winter remains around the freezing point in Scania and the warmest month is July when the average temperature stays around +16°C (Blennow *et al.*, 1999). Average precipitation of this region ranges from 460 to 960 mm year⁻¹ and shows a minimum in February and a maximum in July (Bärring *et al.*, 2003). Most of the plains in this region are covered by the clayey fertile till deposited during the last glaciations. Berglund *et al.* (1991) traced the evidence of agricultural activities in Scania of almost 5000 years back which tell a very long history of more or less continuous changing pattern of landscape. Since 1940s, the merging of farms and cultivation units has changed small-scale farms with dairy production to large units of crop rotation (Bärring *et al.*, 2003). Figure 4 shows the present land cover of Scania and the box inside the image is the study area of the project.

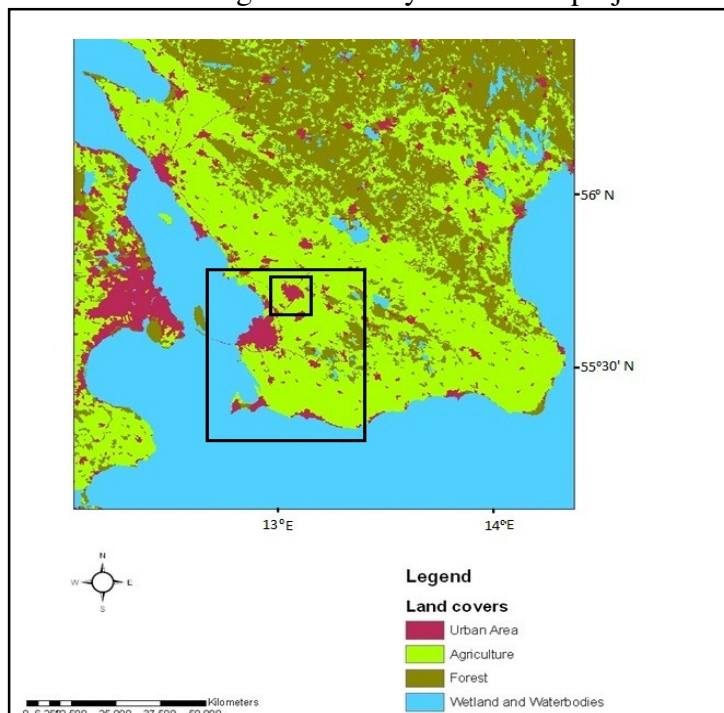


Figure 4: Land cover classes in Skåne, December, 2009. The smaller box in the image indicates the Lund kommun and study area for field visits and the bigger box in the image shows the study area for image based spatial analysis of phenological parameters (Source: EEA, 2010).

The chosen sites were visited at regular interval and rainy and cloudy days were avoided, between April to July, 2010 to take field reading of photosynthetic photon flux density (PPFD) and observed the different stages of crop development. Those field readings were used to analyze PPFD, fraction of intercepted photosynthetically active radiation (FIPAR) and FAPAR for the beginning of the growing season. The sites located in Lund, Arendala and in Åkarp are shown in a SPOT image in Figure 5. The position of the fields were measured with a GPS and validated through the SPOT image by Arc GIS software (Esri, Redlands, USA). The centre coordinate point of the fields were taken to get the MODIS row and column values. The information on the study sites are given in table 2.

Table 2: Location of the study sites. The MODIS rows and columns are from the h18v03 MODIS tile.

| Study sites | Lat/long | MODIS 250m Row/Column | Crop |
|--------------------------|---------------------------------|----------------------------------|-------------|
| Åkarp F1 | lat 55.652230 long 13.126130 | line 2086.43 sample 3554.36 | Barley |
| Åkarp F2 | lat 55.655610 long 13.125410 | line 2084.81 sample 3553.86 | Barley |
| Arendala | lat 55.687370 long 13.266420 | line 2069.56 sample 3589.13 | Wheat |
| Norra Faladen | lat 55.730550 long 13.217650 | line 2048.84 sample 3571.98 | Wheat |

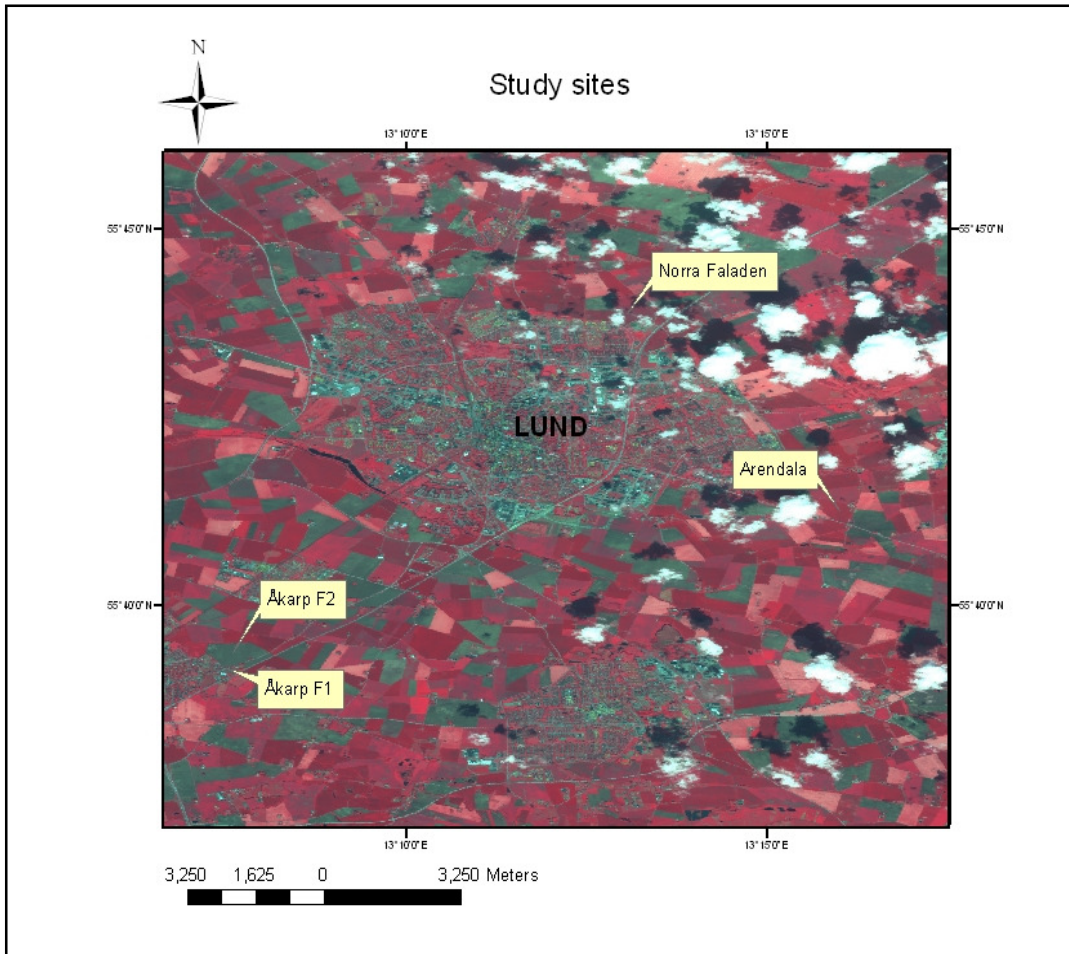


Figure 5: Location of the study sites in a SPOT image on 20th May,09.(Source: SACCESS, 2009)

The crop fields were selected according to their size for at least 250 by 250 meters because the spatial resolution of the MODIS data products used in this study (MOD09Q1) is 250 meters. The bus route was the only way to the sites for me, so crop fields were found on the way to Dalby and Åkarp. The first two sites were in Åkarp F1 and Åkarp F2 was used for traditional crops like barley. Arendala is an agricultural region and the site is also used to grow wheat crop. The fourth site, Norra Faladen was used to grow wheat crop.

3.2 Measurements of photosynthetic photon flux density

3.2.a) TRAC reading from fields:

The TRAC (Tracing Radiation and Architecture of Canopies) (Canada Centre for Remote Sensing, Canada) was used to measure photosynthetic photon flux density (PPFD) along transect of 100 m for all the study sites. This instrument measures incoming and outgoing radiation at high frequency. In data logging mode, it takes reading 32 times per second. It has three sensors (Figure 6.a) which are able to take reading serially in $\mu\text{mol s}^{-1} \text{m}^{-2}$.

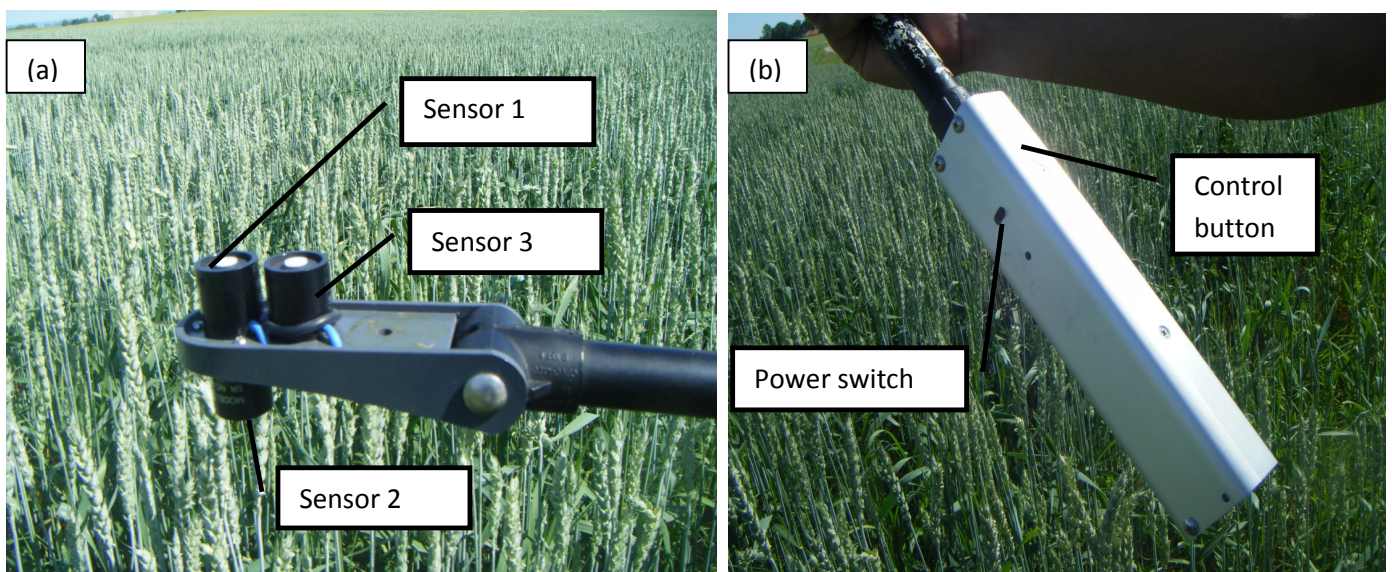


Figure 6: a) The three sensors of TRAC, b) Power switch and control button.

A power switch (Figure 6.b) controls the power to all components of the system except the memory and control button (Figure 6.b) controls the operating mode when the power is on. This power button is also used as distance /time markers. When the control button was switched on the reading from the crop fields were taken by walking in the fields and the instruments was kept horizontal parallel position to the top of canopy. Figure 7 shows the measurement of TRAC reading taken in the agricultural field at Norra Faladen (left image) and the measured fraction of reflected PPFD (PPFD-r) and incoming PPFD (PPFD-i) for that transect.

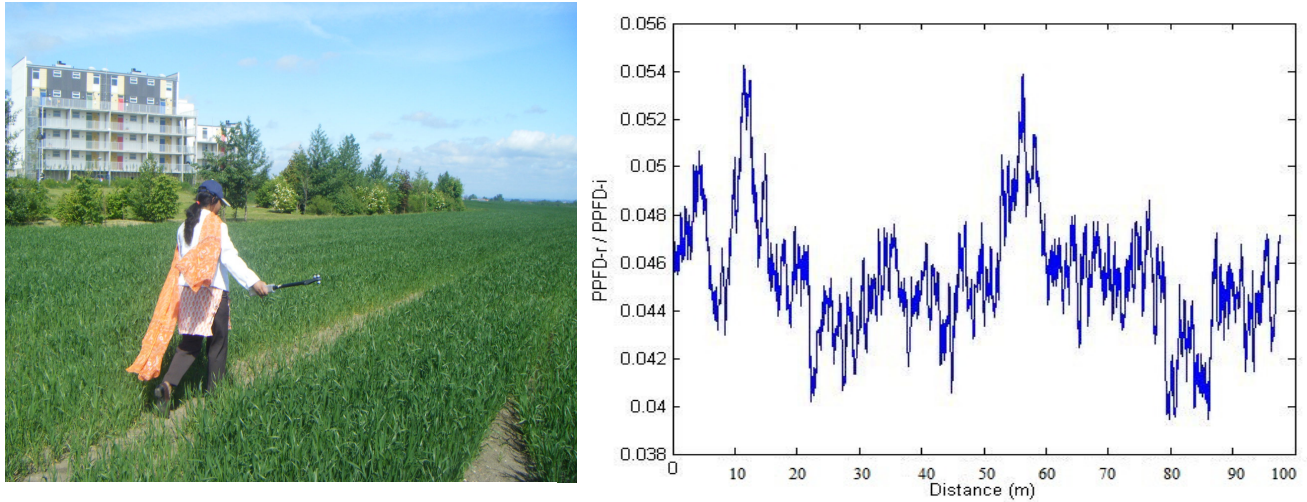


Figure 7: Left: Using TRAC in a wheat field. Right: the reading from TRAC calculated as fraction of reflected PPFD and incoming PPFD for 100 m transect in Norra Faladen site on 8th July, 2010.

After gathering all data sets for all fields, the computation of PPFD_R (Reflected photosynthetic photon flux density) and PPFD_I (Incoming photosynthetic photon flux density) were done by excel and FIPAR was estimated using the formula in equation 4.

$$\text{FIPAR} = 1 - \text{PPFD}_R / \text{PPFD}_I \quad (4)$$

Here FIPAR is Fraction of intercepted photosynthetically active radiation in the fields.

3.2.b) Fraction of green portion in the site:

Several photographs from each site on the transect of TRAC were taken on all visits. The photographs were taken almost two feet above of the top of crops and at nadir view. Those photographs were analyzed through IDRISI Andes software (Clark University, Worcester, USA) to get the proportion of green (vegetation cover) and non green (soil or without vegetation cover) area at the site. First the JPEG images were imported in IDRISI and were separated in 3 bands. Then band 1 was subtracted from band 2 and in reclass function the pixel values were categorized in two parts, 1 as vegetation part and 0 as non vegetation part. Numeric proportion of the green and non green part was obtained from histogram option. Figure 8 shows the photograph taken from field in (a) and the area of the photograph were reclassified in two categories, Vegetation cover and non vegetation cover in (b).

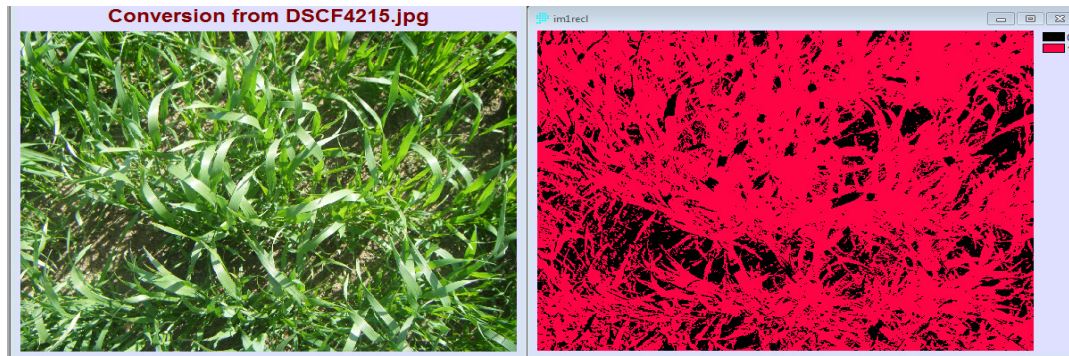


Figure 8: Photograph taken on 17th June,2010 on Norra Faladen site, (a)Photograph on field, (b) Reclass of the photograph in IDRISI Andes as green '1' and non green'0'.

Using the formula from Schubert *et al.* (2010), the value of FAPAR calculated by the multiplication of FIPAR and green portion of the site, A_g .

$$FAPAR \approx A_g * FIPAR \quad (5)$$

It was the main principle of the field work to get FAPAR from field observation.

These FAPAR values from all study sites were used to follow the spring green up of the crops and compared with the MODIS vegetation indices (VI).

3.3 Time series and statistical analysis

Downloaded MODIS images were converted into binary format of NDVI, WDRVI and Combined Quality data for the four pixels of four study sites. The lists of NDVI and WDRVI values for 4 pixels in each image were extracted for 11 years of time series. Then these VI values were stored in excel sheet and arranged according to dates.

TIMESAT is a software package and was developed for estimating growing seasons from satellite time-series, as well as for computing phenological metrics from the data (Jönsson and Eklundh 2002, 2003, 2004, Eklundh and Jönsson 2003). This software is able to fit smooth mathematical functions to time-series of noisy satellite data and key phenological matrices are also possible to be extracted for each image pixel. So the extracted indices values were run in TIMESAT to show graphical pattern of time-series. Figure 8 shows the menu system of TIMESAT software, where TIMESAT-GUI was used to extract the time-series for different indexes. Each index was represented with a weight value to specify its importance or quality. Weight assigned in TIMESAT graphical user interface (GUI) for the NDVI and WDRVI to weight the function fitting in TIMESAT. The quality indices were stored in binary image files of the same data type and formatted as NDVI or WDRVI data type. The weights are shown in Table 3.

Table 3: The weight for the quality indices in TIMESAT- GUI.

| File values | Weight |
|-------------|--------|
| 2 | 1 |
| 1 | 0.5 |
| 0 | 0.01 |

There were several fits in data plotting part of TIMESAT Graphical User Interface (GUI) to make smoother time-series from the pixels of an area for VIs and Savitsky-Golay matches the series for the best fit among all. Seasonality data from GUI (see figure 9, right) were extracted to analyze different phenological parameters for four pixels of the study sites. The right image in figure 9 shows the phenological parameters that can be extracted by TIMESAT software. Those parameters were extracted in ASCII format, and later image based seasonality information extracted by different processes (e.g. TSF process and TSF_seas2img) in TIMESAT. In TSF_process, all the index values are calculated in fortran mode and in TSF_seas2img, the seasonal parameters are calculated for the image). Those images were used to establish spatial changes of the crop phenology between 2001 and 2009 for south western Skåne. Seasonality data in images were extracted only for pixels those are used as agricultural land and that image was used as mask for image output.

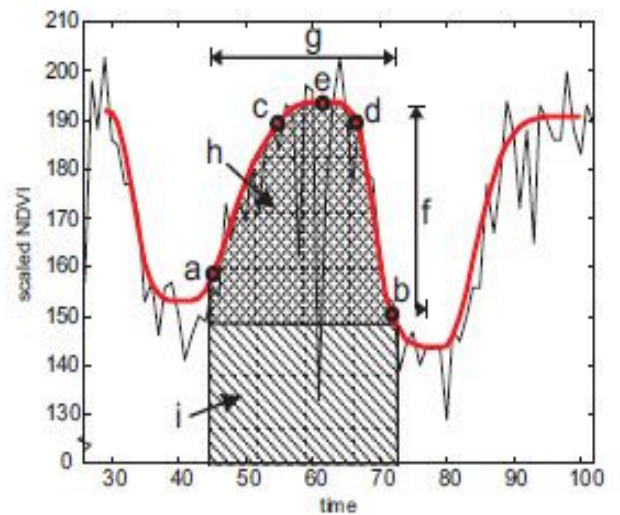
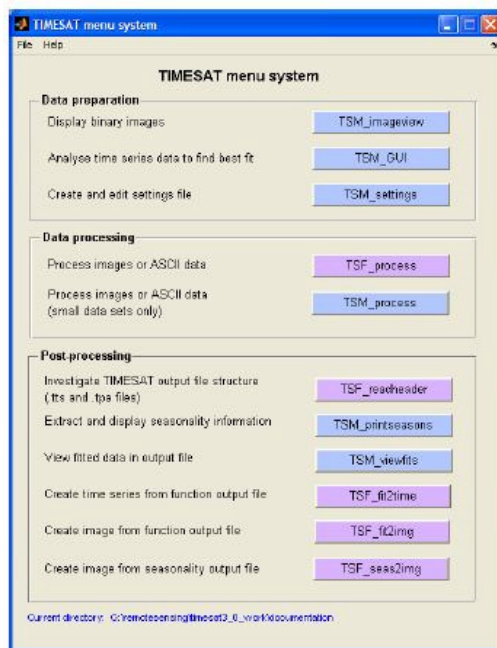


Figure 9: Left: TIMESAT menu system. Right: Seasonality information computed in TIMESAT: (a) beginning of season, (b) end of season, (c) left 90% level, (d) right 90% level, (e) peak, (f) amplitude, (g) length of season, (h) integral over growing season giving area between fitted function and average of left and right minimum values, (i) integral over growing season giving area between fitted function and zero level (Source: Jönsson & Eklundh, 2004).

4. Results

4.1 FAPAR observation from field

The fraction of absorbed PAR (FAPAR) as estimated in two barley fields in Åkarp and two wheat fields in Arendala and Norra Faladen, were in increasing trend for the beginning of the growing season. Figure 10 shows the increasing trend of FAPAR for five visits in each site.

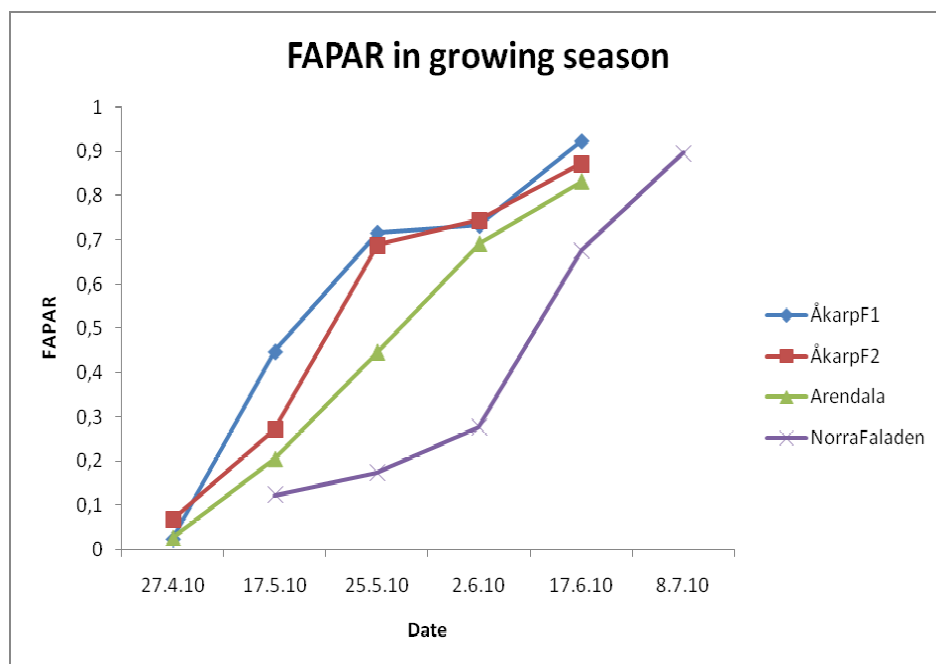


Figure 10: FAPAR for all study sites.

The relationship between vegetation indexes and FAPAR were investigated in different studies for forest cover. Chen (1996) drew a Linear relationship between NDVI and FAPAR for non-forested ecosystems which is not that much strong ($R^2 = 0.56$) whereas Goward *et al.* (1994) found much stronger relationship ($R^2 = 0.99$) between AVHRR NDVI and FIPAR for forested sites in Oregon, USA. The NDVI-FAPAR relationship is near-linear rather than linear as NDVI saturates at high leaf area index (LAI) values and PAR absorption increases beyond this point (Olofsson & Eklundh, 2007). There were lacks of study to measure FAPAR directly from the agricultural fields. So the FAPAR values were measured for two types of crops to investigate the relationship with MODIS derived vegetation indices.

4.2 Extraction of MODIS NDVI and WDRVI through TIMESAT in ASCII format

MODIS images were used to extract NDVI and WDRVI from 2000 to until 18th June 2010. TIMESAT requires data of full years to run for seasonality data or draw time-series. Figure 11 shows the recent images on south west Skåne which were used to extract ASCII and image values of VIs. Whenever the indices were extracted the data for rest of the year were copied after the data on 18th June, 2010 and completed data set of 11 years for analysis. Savitzky-Golay fit were chosen to fit the time series data and for most of the cases TIMESAT was able to cover the whole season except for one or two years in the whole time-series. This kind of seasonal data is problematic to show real phenology, such as small integral or length of season.

Figure 12 shows the NDVI values in 11years (2000 to 2010) of time-series for study sites and Åkarp F1 field is only error free time series which has start and end of season for all the years in time-series. Figure 13 shows the WDRVI values for 11 years of time-series for all study sites and like NDVI data these series have missing seasons which are not included in the TIMESAT defined seasons. So the seasonality data on end of season, length of season and small integral of season did not cover all crop phenology for the second season of the years in few cases in the time series.

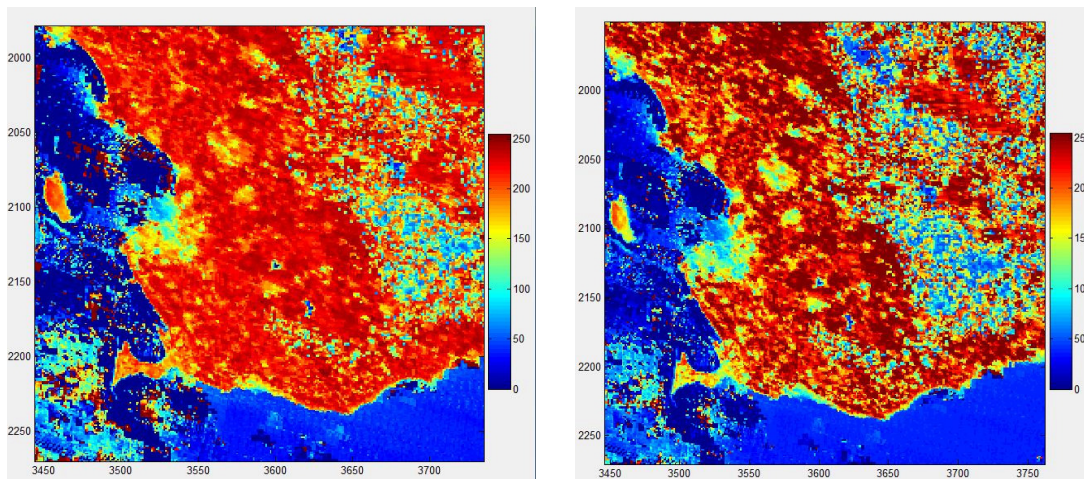


Figure 11: South west Skåne in a MODIS image on 18th June, 2010. Left: NDVI values in the area and right: WDRVI values in the area.

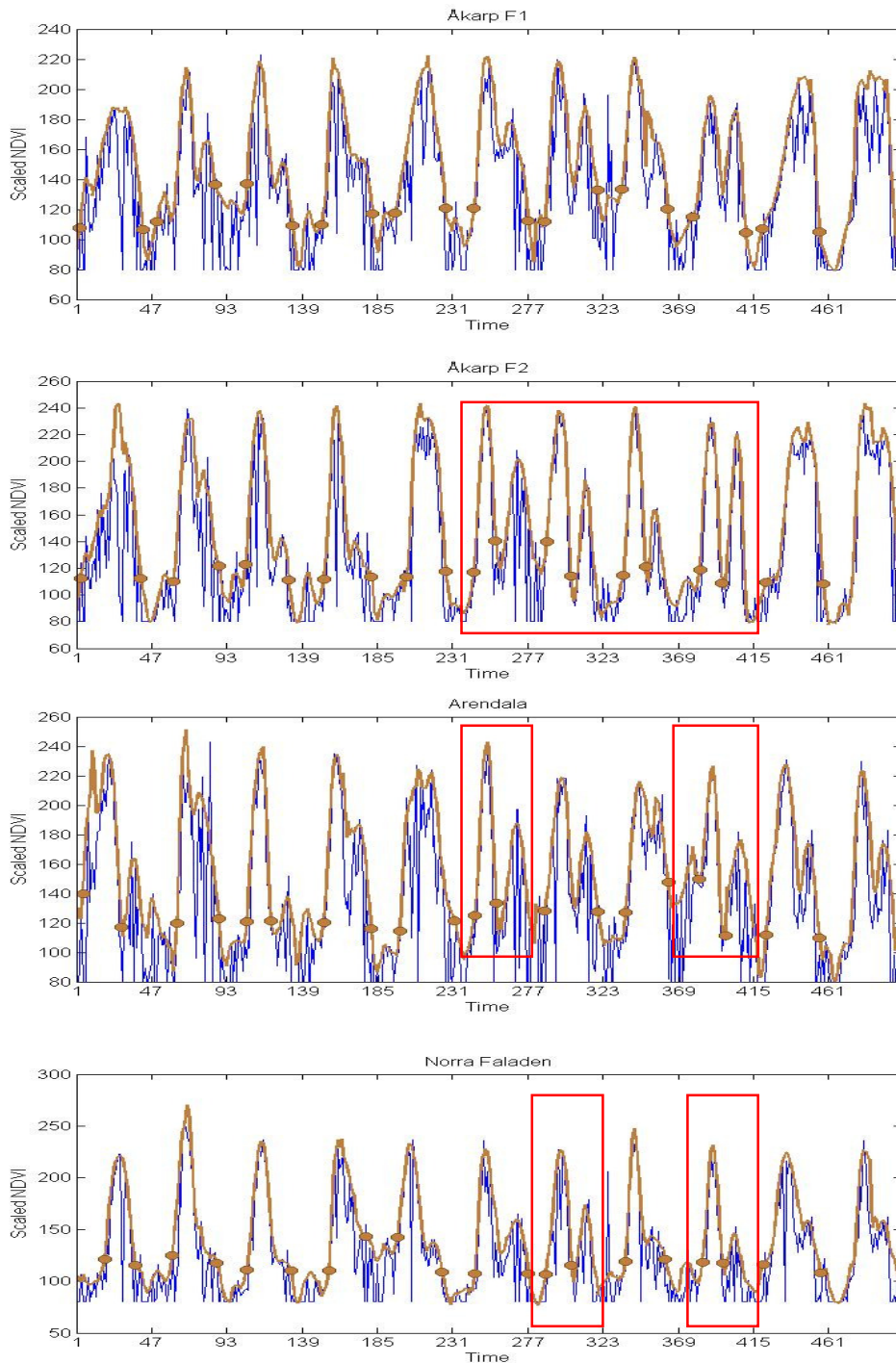


Figure 12: Scaled NDVI values on four study sites from 2000 to 2010. Blue line indicates time-series that was extracted from MODIS, brown line is TIMESAT derived fitted line from Savitzky Golay filtering and the brown circles indicate the start and end of growing season. The red boxes show the missing of second season from fitted growing season.

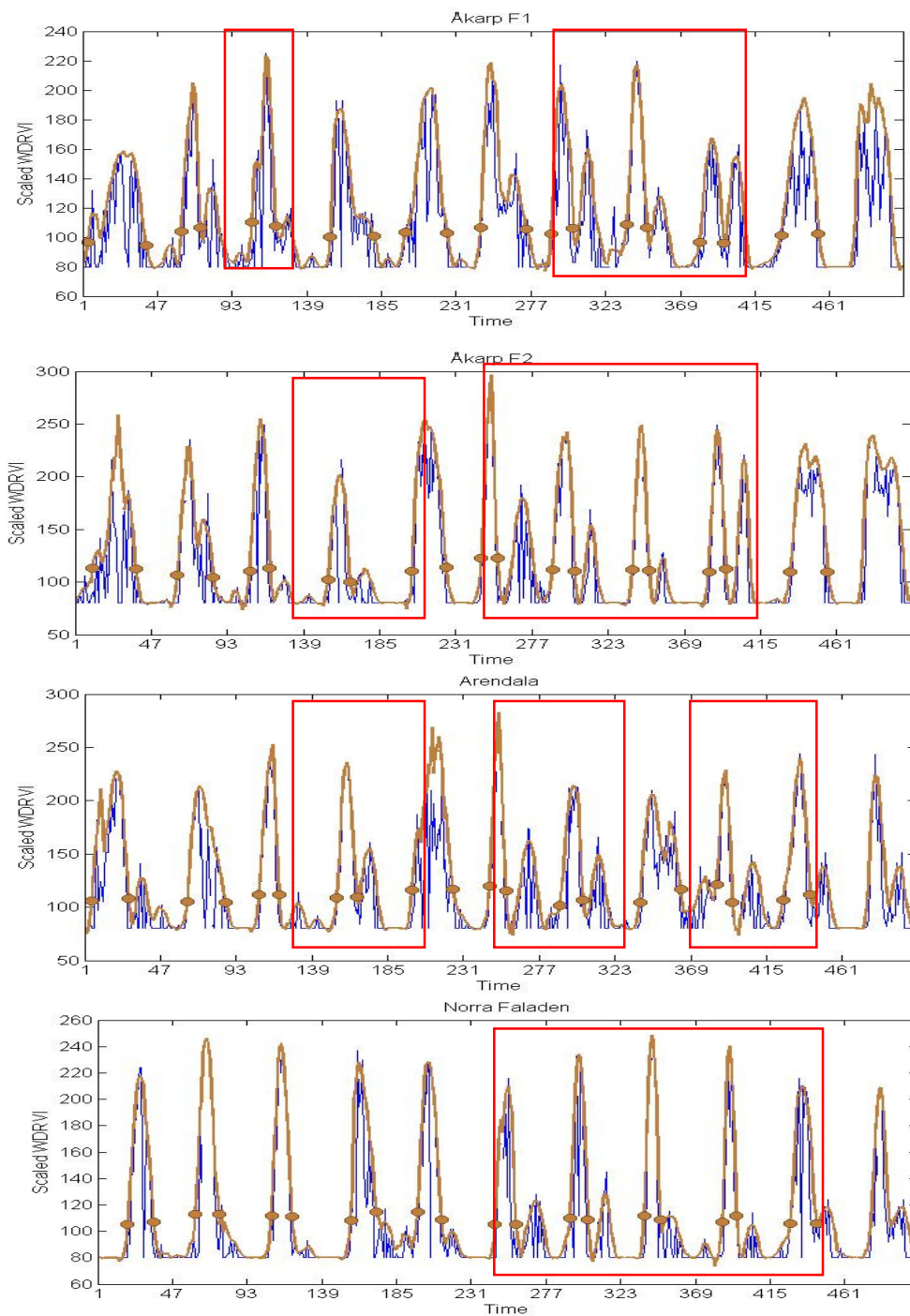


Figure 13: Scaled WDRVI values on four study sites from 2000 to 2010. Blue line indicates time-series that was extracted from MODIS, brown line is TIMESAT derived fitted line from Savitzky Golay filtering and the brown circles indicate the start and end of growing season. The red boxes show the missing of second season from fitted growing season.

TIMESAT shows scaled values for the indexes in graphics which converted by the following equations,

$$\text{NDVI} = (\text{DN} - 42.5) / 212.5 \quad (6)$$

$$\text{WDRVI} = (\text{DN} - 153.0) / 170 \quad (7)$$

Here DN is the digital no. or scaled value of the index.

Time-series data were used to get NDVI and WDRVI values for growing season of 2010 and those were directly compared with the FAPAR obtained from fields. According to Jönsson & Eklundh (2003) Savitzky-Golay algorithm is faster than other and never fails to cover but in pixel based study it seemed some problems in coverage of the dual seasons. In this section length, peak value, amplitude and small integral of seasons were analysed among all parameters. According to NDVI time-series the average length of the season for the study sites was 208 days, the average peak value was 229.52 means the NDVI average in the region was generally 0.8 (using equation 6). The average amplitude of the growing season was 138 and small integral was 2214.

When the time-series from WDRVI was analyzed, seasonality information extracted was smaller than the NDVI time-series. Average length of the seasons was 128 days, average peak value was 0.32, and seasonal amplitude 118 and small integral was 1598.

Figure 14 shows length of the seasons derived from NDVI and WDRVI from all study sites and overall trend of the length is in decreasing trend (though some cases have missing dual seasons). It is an important parameter because the longer length of season indicates the sequestration of carbon will take place for longer time period. The lowest length of the season from NDVI time-series was 100 days in 2005 (when only one season was detected by TIMESAT) and the highest reached at 300 days in 2000. Whether in WDRVI time-series the length of the seasons varied lowest at 70 (in 2005, the reason was same as NDVI) and highest at almost 250 days. The reason of the changes of length could be the result of different crop for the different year or for some climatic factors.

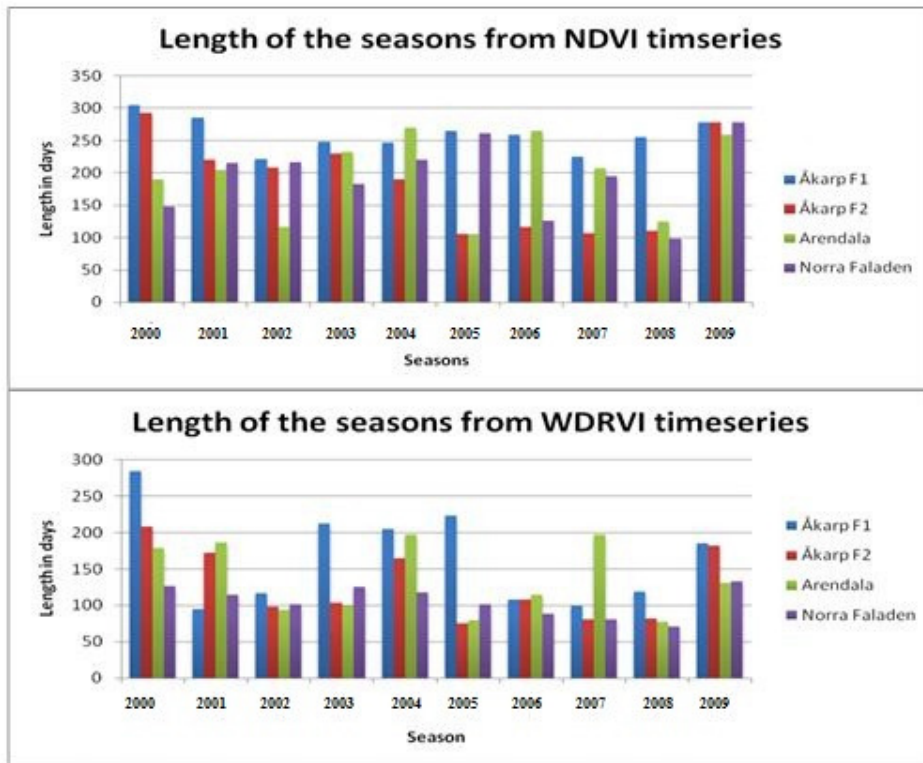


Figure 14: Length of seasons from NDVI and WDRVI.

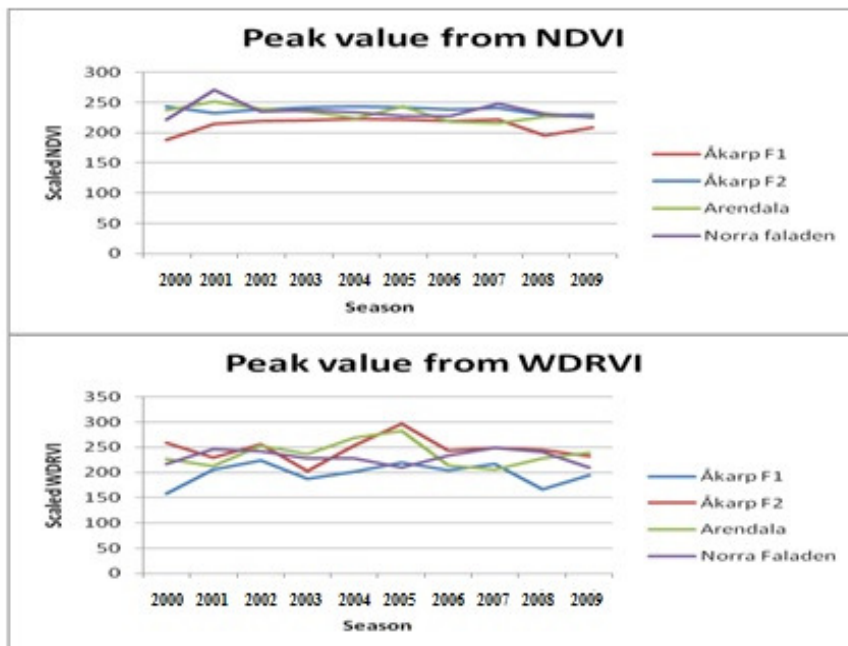


Figure 15: Peak value from NDVI and WDRVI.

Peak value of VIs is also an important seasonality parameter as it indicates the maximum value of index in a season. Figure 15 shows the peak value in NDVI time-series varies between 200 and 250 scaled NDVI and from WDRVI those values vary between 150 and 300 scaled values.

The amplitude of a season can be obtained from the difference between the peak value and the average of the left and right minimum values (Jönsson and Eklundth, 2004). Figure 16 shows the amplitude values from both NDVI and WDRVI for all study areas and for all the cases the amplitude of the seasons are slightly decreasing trend.

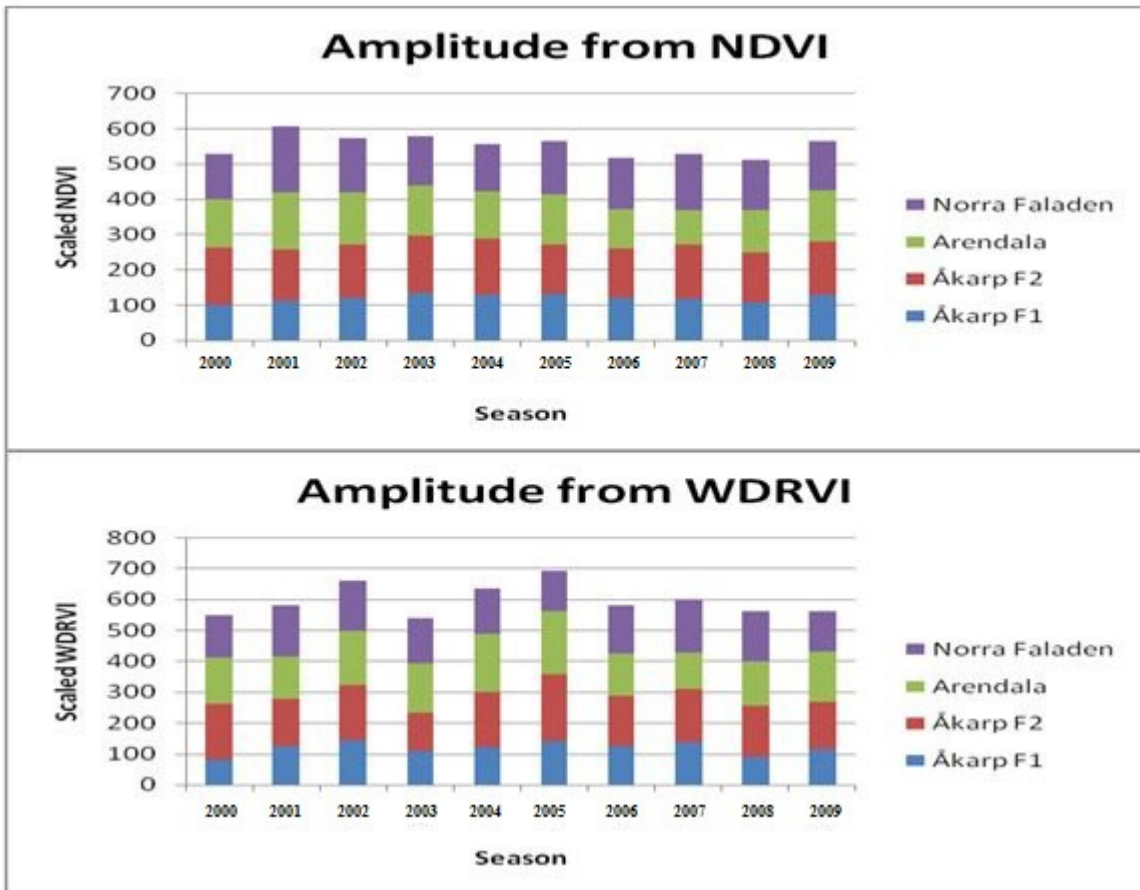


Figure 16: Amplitude of seasons from NDVI and WDRVI.

Jönsson and Eklundh (2004) estimated production of the seasonally dominant vegetation by computing the integrated NDVI over the growing season which is known as small integral and belongs between start and end of the season. This kind of annual integrated NDVI was used in several studies as a measure of net primary production (NPP) (Running and Nemani, 1988; Goward and Dye, 1987; Ruimy *et al.*, 1994).

Figure 17 shows the small integral from the study sites and from NDVI it varied 1200 to 3500 and from WDRVI it varied almost 900 to 3000. As this value depends on the coverage of the whole growing season of a year it is important to count all season in a year but TIMESAT showed some limitation on crops which was failed to include the second season in its seasonality.

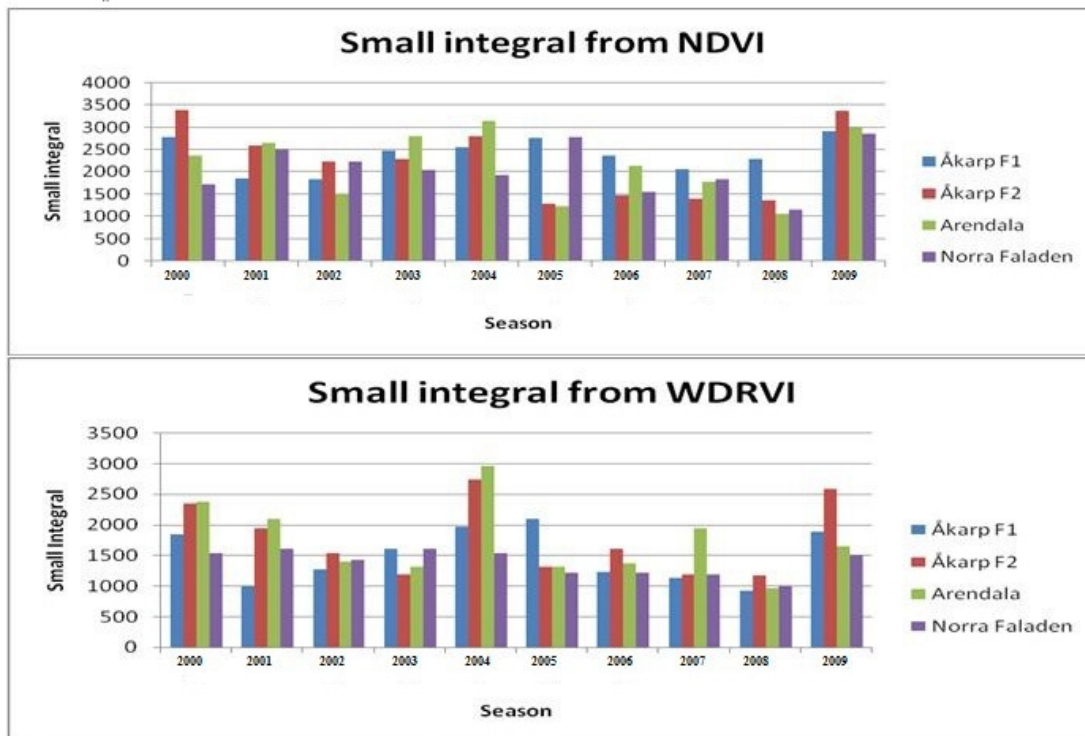


Figure 17: Small integral of seasons from NDVI and WDRVI.

4.3 Relationship between FAPAR and MODIS NDVI

The observed FAPAR values were modeled with MODIS NDVI values extracted through TIMESAT and it showed the good correlation in case of barley and wheat fields.

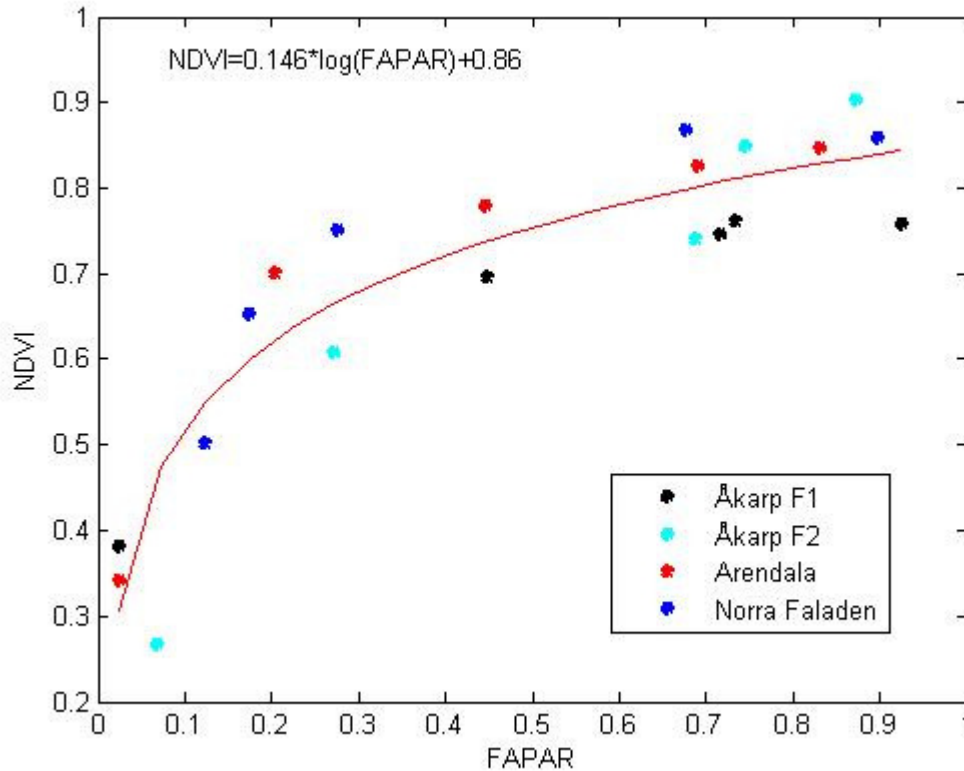


Figure 18: The relationship between FAPAR and NDVI.

Figure 18 shows the scatter plots of measured FAPAR and TIMESAT adjusted NDVI values for all study sites and the result of logarithmic fit was

$$NDVI = 0.146 * \log (FAPAR) + 0.86 \quad (8)$$

with $R^2 = 0.71$.

Xiao *et al.* (2004) also distinguished between the photosynthetically-active and non-photosynthetically active components of canopy absorbed radiation and found close correlation between NDVI and total canopy FAPAR. Asrar *et al.* (1984), Goward *et al.* (1992) and Viña & Gitelson (2005) observed a significant decrease in the sensitivity of NDVI to FAPAR occur when FAPAR exceeds 0.7 which also visible in figure 17 and the values were almost in saturating trend at NDVI levels at 0.7.

4.4 Relationship between FAPAR and MODIS WDRVI

Figure 19 shows the nonlinear relationship between fields estimated FAPAR and MODIS derived WDRVI for all study sites and the logarithmic fit was

$$\text{WDRVI} = 0.211 \cdot \log(\text{FAPAR}) + 0.345 \quad (9)$$

with $R^2 = 0.74$.

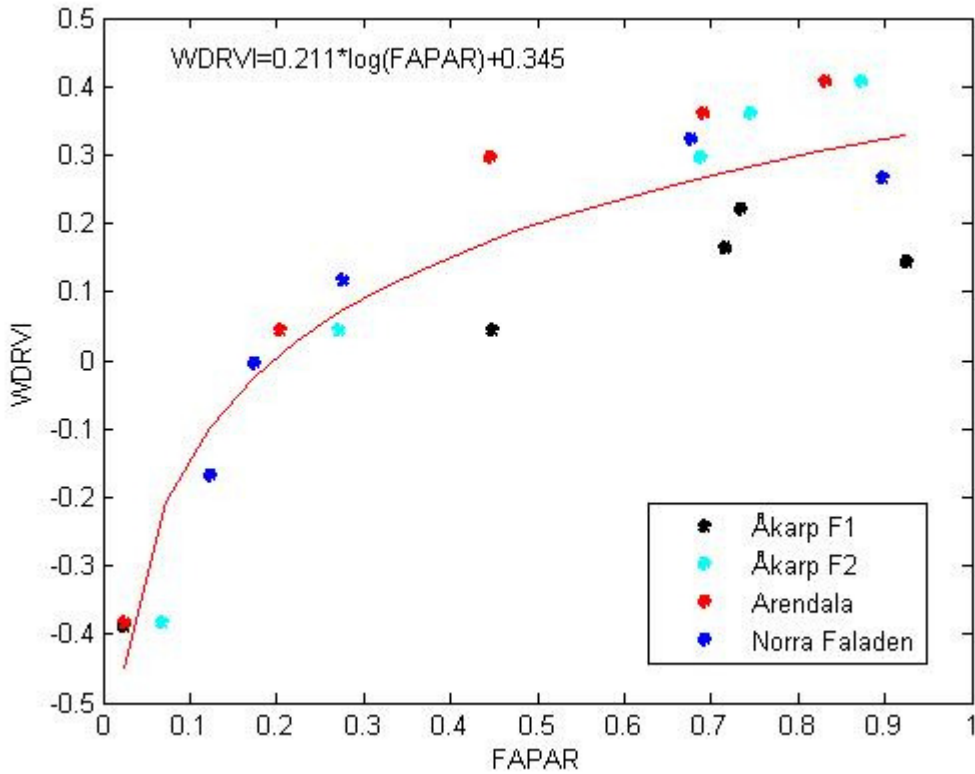


Figure 19: The relationship between FAPAR and WDRVI.

According to equation 9, the overall WDRVI from crops explains 74% of the variation in FAPAR and significance level 0.00 indicate the data is believable.

4.5 Seasonality analysis from images

4.5. a) Length of season

Satellite images are good representative to analyze spatial changes of phenological parameters and as well as vegetation indices. Climate of a region determines the suitable cropping time for an agricultural region. As the study area remains under snow for a certain period of time in every year, so start of sowing seeds in spring depends on the regional climatic conditions. Generally the season begins at the end of March in most of the places but in some cases season starts later.

Figure 20 shows the variation of length of season in south western Skåne from NDVI time-series. The increase of the length of season significantly varied in the NDVI time-series from year to year for most of the parts in the area. If we analyze the images on 2001 and 2002 it is clearly visible that there were increase of length in most of the part of the region and the higher increase occurred at the north eastern part of the images mainly beside the lake and forest cover. In 2003 the length of the season decreased in some part of the area beside coast than 2002 but it again increased in 2004. 2005 showed the highest number of pixels than other images with increased length and it reached maximum of 280days in a whole year. Among all images of the time-series, 2005 had higher increase of seasonal length. Length of season from 2006, 2007 and 2008 had almost same pattern and varied very little in the area beside southern coast and forest areas. In 2009 length of season for some places decreased 280 days to 240 days mainly at the eastern part of the area, but there was increasing pattern of length mainly the middle part of the whole area.

Figure 21 shows the pattern of the length of season from WDRVI time-series in south west Skåne. In 2003 the maximum length reached 320 days for few areas in the eastern part and the overall increase of length of season was visible than 2001. The maximum length of season decreased to 240 days in 2003 and the pattern were almost same for 2004, 2005 and 2007. Among those years 2004 and 2008 shows more variation of spatial disparity for length of season. In 2009 the maximum length of season reached 240 days those were higher in the previous years, indicates the decreasing trend of seasonal length for time being.

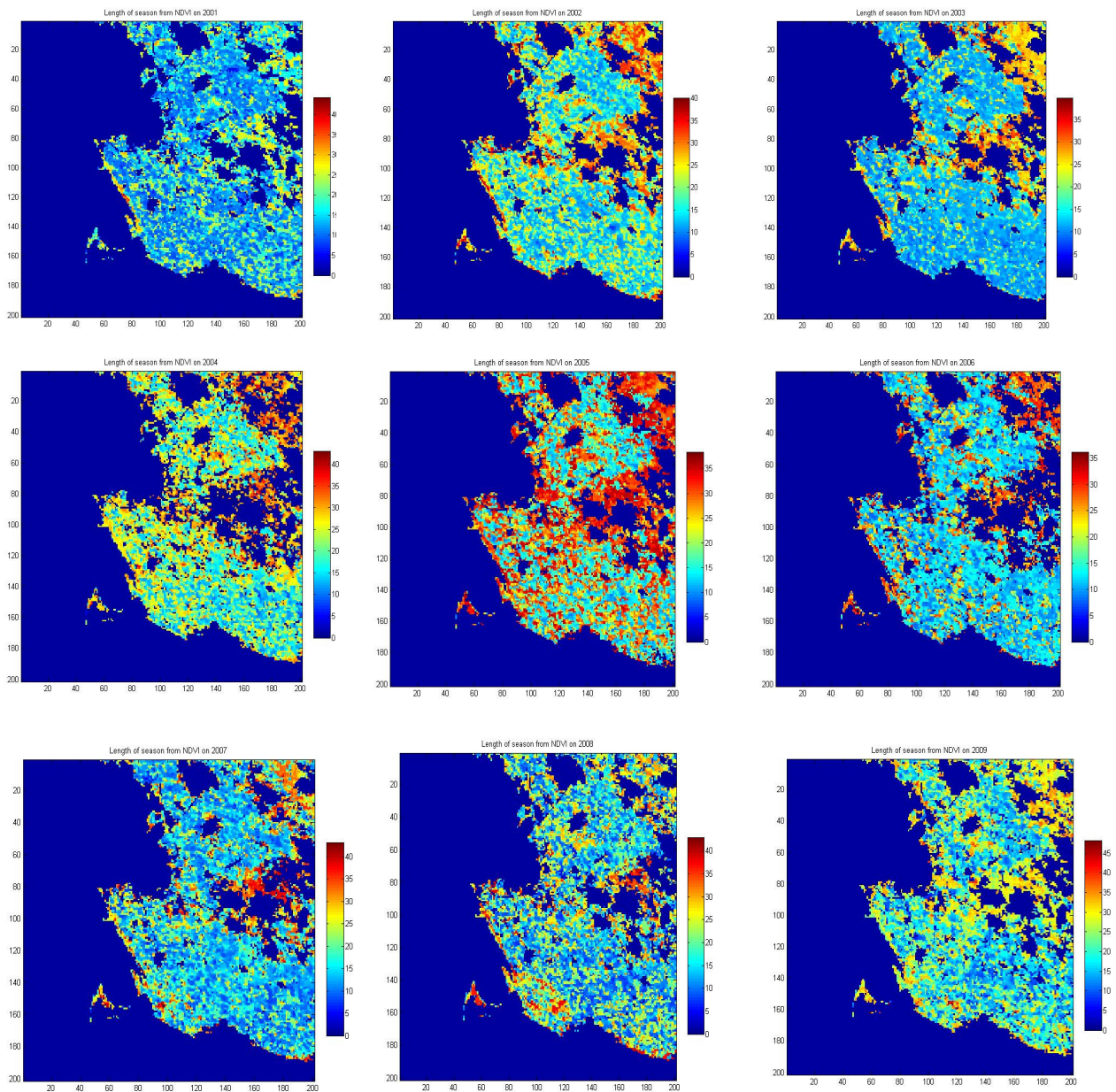


Figure 20: Length of season from NDVI time-series from 2001 to 2009. The index values have to be multiplied by 8 to get the length of season in days.

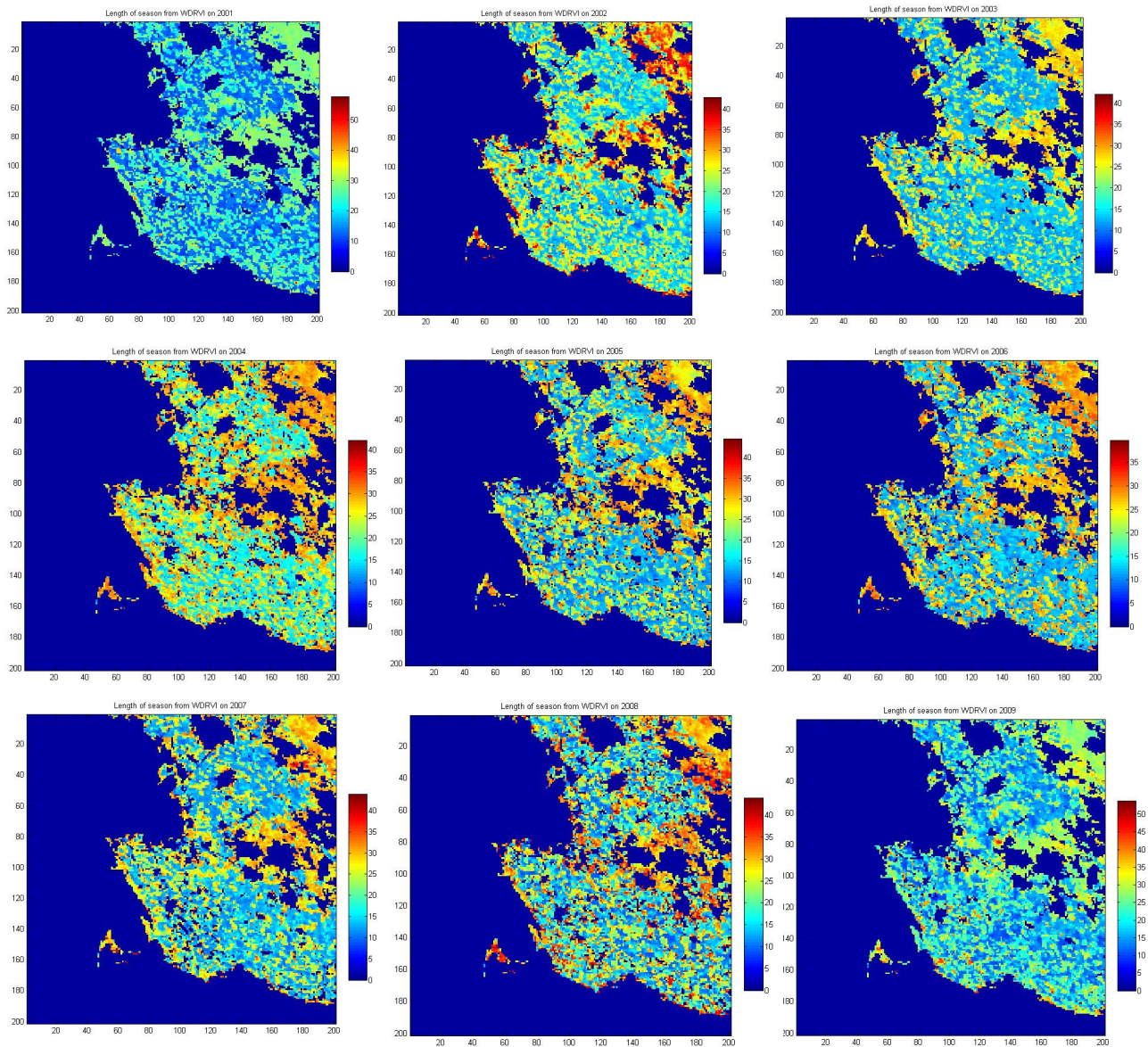


Figure 21: Length of season from WDRVI time-series from 2001 to 2009. . The index values have to be multiplied by 8 to get the length of season in days.

4.5. b) Amplitude of season

Amplitude of season is an important parameter and figure 22 shows amplitude of season from 2001 to 2009 from NDVI time-series. From the images between 2001 and 2009 the high amplitude was visible in 2003, 2004 and 2005. The maximum value of amplitude varied 200 to 250 for those three years which were at the eastern part of the region. After 2005, the amplitude values decreased in most of the part of south western Skåne and the spatial pattern of this

parameter was almost same for 2006, 2007 and 2008. In 2009 the amplitude was again increased in all over the area and the maximum value reached in between 200 to 230.

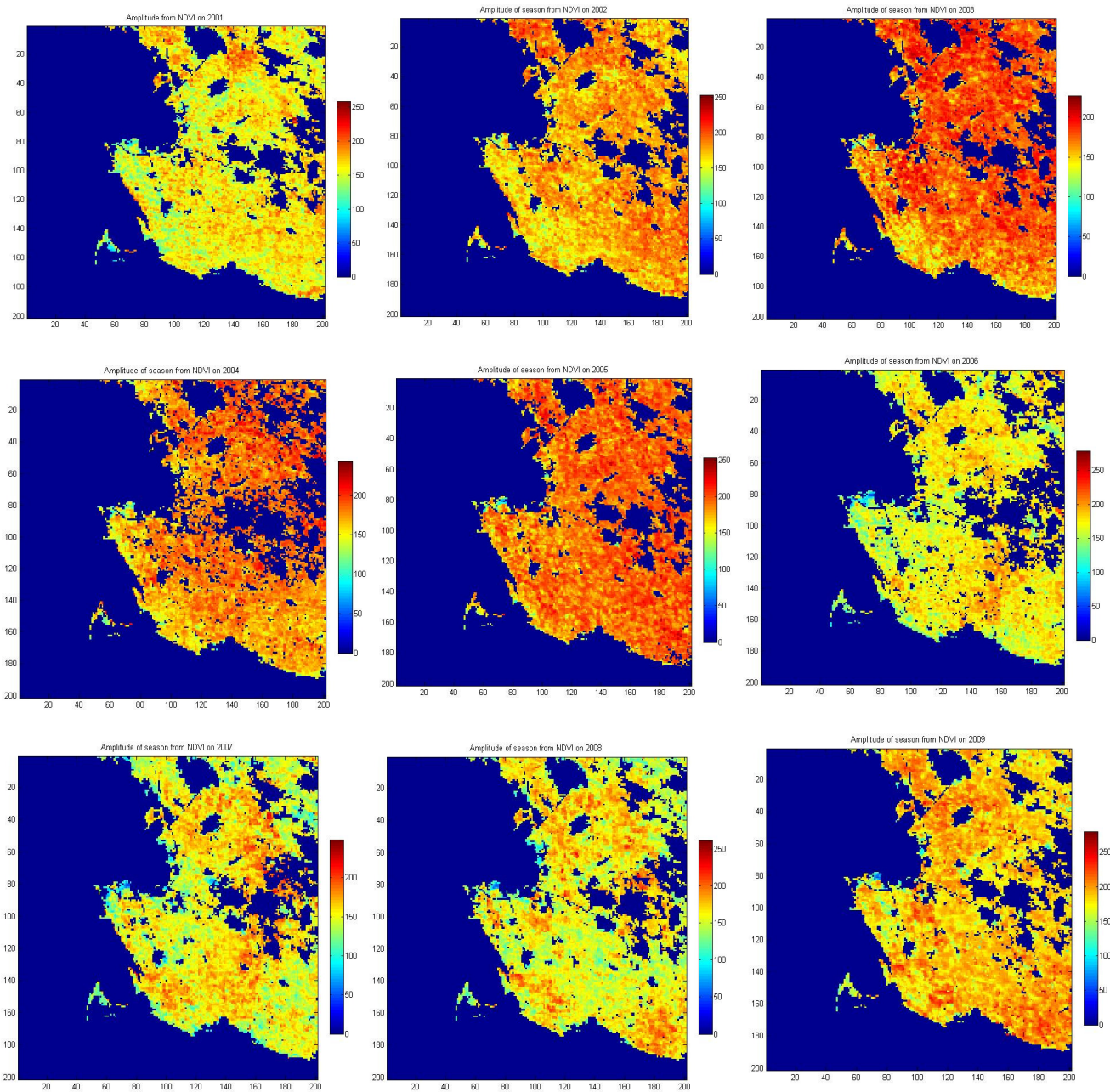


Figure 22: Amplitude of season from NDVI time-series.

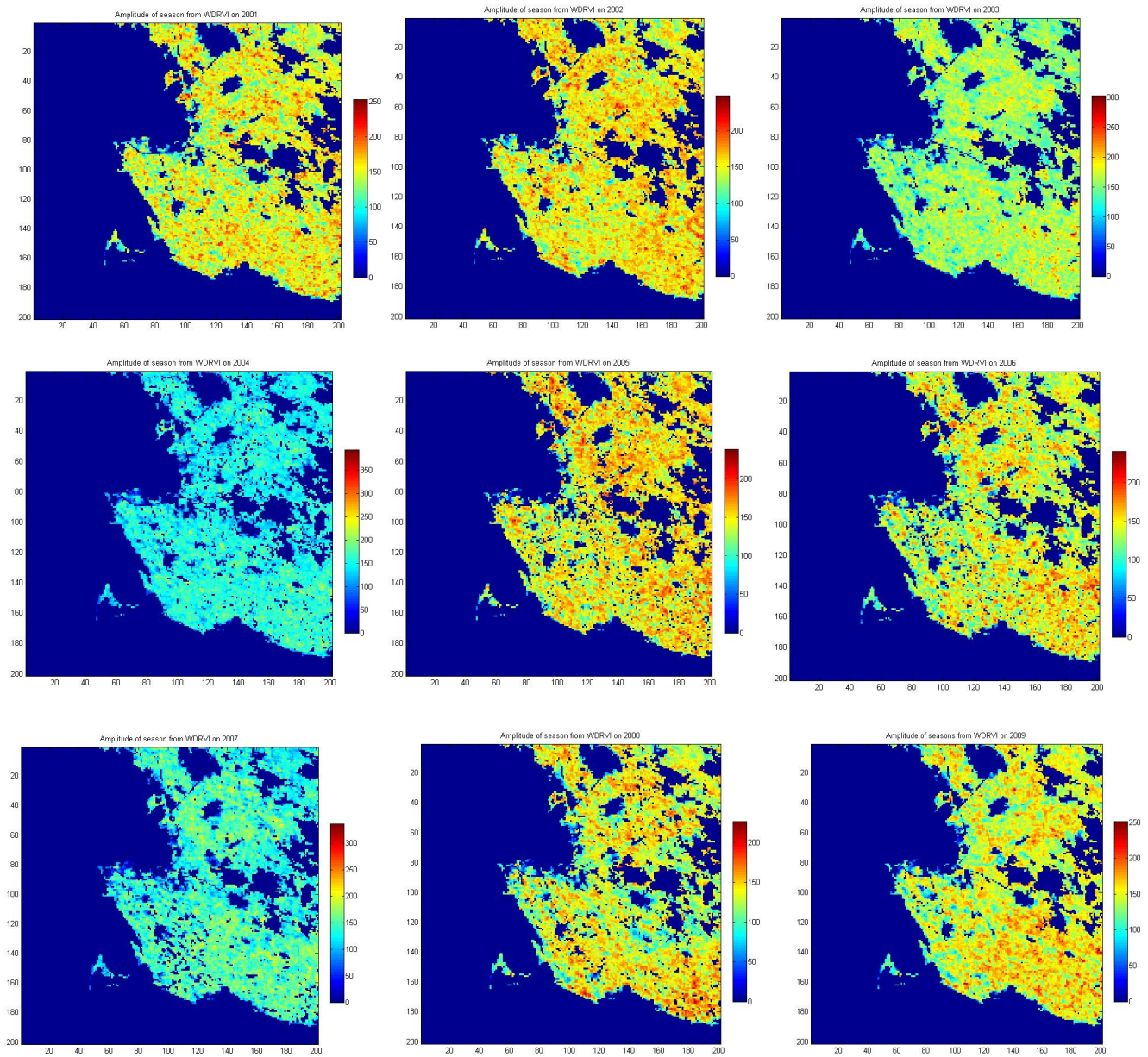


Figure 23: Amplitude of season from WDRVI time-series.

In case of WDRVI time-series (figure 23) the amplitude of season were 150 to 200 in most of the area in 2001, 2002, 2003, 2004 and 2009. The amplitude varied 130 to 180 for rest of the years (e.g. 2005, 2006, 2007, 2008). The changes of seasonal amplitude varied all over the area, and there were no distinct spatial pattern of change of amplitude values.

4.5.c) Small integral of season

There were significant increases of small integral from NDVI time-series in 2002, 2003, 2005 and 2009 (figure 24). Most of the area in the south west Skåne in figure 24 shows the increase of productivity and the average increase was 4000 for those years. The spatial pattern of small integral varied in different positions, e.g. small integral increased at the middle to eastern part of the images. There were similarities within the images of 2004 and 2006 in case of spatial pattern of that parameter. Some places were displayed as missing parameter values beside the lake and forest whether the higher values were also observed in that area.

Figure 25 shows small integral of season from WDRVI time-series where 2001, 2002 and 2003 had almost same spatial pattern and higher parameter value (2400-3500) were at the north and middle part of the images. In 2004, small integral had increased at most of the region and the average value was 2500. There were almost similar pattern found in 2005, 2006 2007 and 2008. For those images the higher values were in the north east part of the area which was almost 3200.

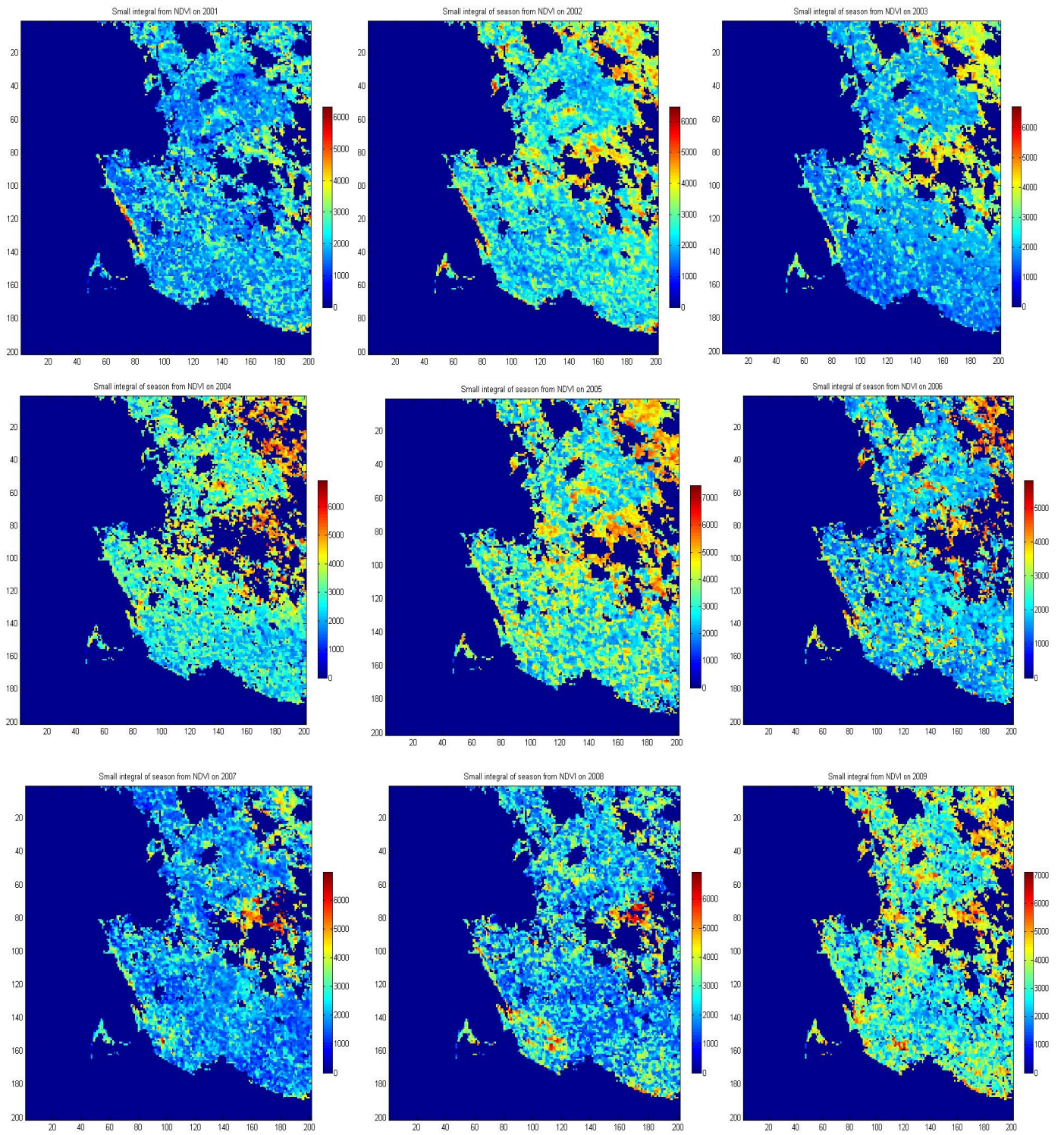


Figure 24: Small integral of season from NDVI time-series.

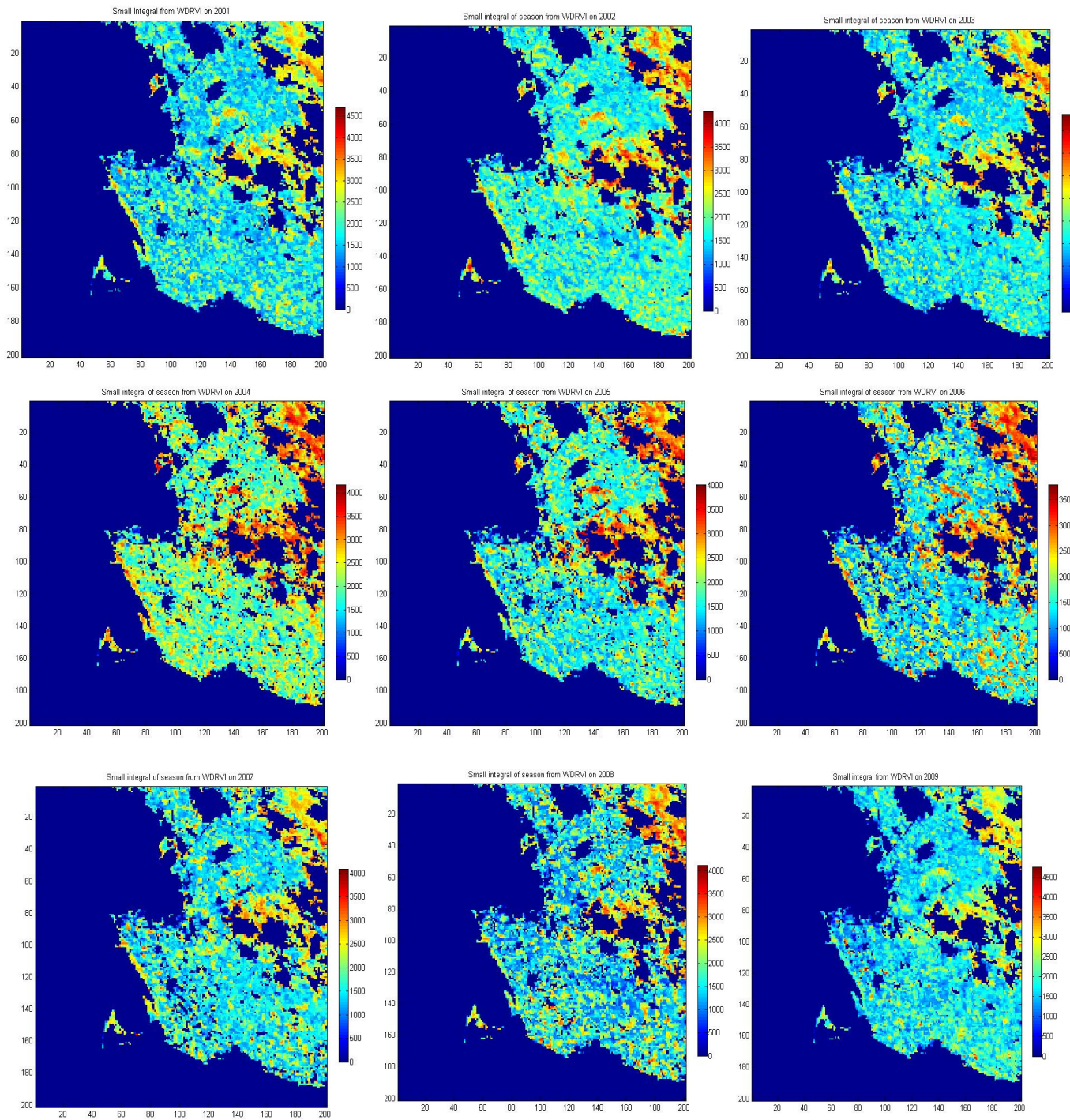


Figure 25: Small integral of season from WDRVI time-series.

5. Discussion

5.1. Discussion on project result

Crops are one of the most important dominating land cover in Skåne and seasonality information from that area should be given more importance. The increasing trend of population created an ecological crisis in the 18th century because of deforestation and cultivation of new land (Mattsson, 1987). Southern Sweden became a fertile land by the glacier deposits and suitable for agricultural practices, is one of the best fertile land in Europe (discussion with Jonas Åkerman, 2010). Remote sensing can be the excellent tool for monitoring crop resources of the region and MODIS images could be one of them, which can be use as reliable data source. So, not only to analyze the carbon budget, but also for discussion of phenological patterns, vegetation indexes are the best indicator.

TIMESAT is a useful tool to extract time-series of different VIs and seasonality information from agricultural field. It is possible to produce VI values in TIMESAT for each pixel and as well as for the whole image. So the spatial analysis of phenology becomes easier.

Field observation of FAPAR (figure 9) showed the increase of spring green up day by day for all the study sites, so TRAC was able to measure hopefully correct PPF_D from solar radiation. So with green up of crop the FAPAR also increased for all the observation, though the TRAC reading gave problematic values in cloudy and windy weather. That kind of result can be useful to measure GPP of that crop field by equation-3, when the value of PAR and light use efficiency is known (measured from flux data).

TIMESAT derived time-series show the index values in ASCII format for 11 years but there were some problems for dual seasons in a year, which seemed challenging to include both seasons in seasonality information. The red boxes in figure 12 and 13 show the problems in missing seasons in NDVI and WDRVI time-series. Though the amplitude and length of those second seasons are sometimes very small, but those should be included in the season as the value of length and small integral of a season will vary by the parameters of second seasons. So in that case TIMESAT was not completely able to extract actual seasonal parameters for crop.

FAPAR vs. NDVI and WDRVI relationship found to be non- linear and strong in case of MODIS derived VIs and field observed FAPAR. The correlation between FAPAR and these two VIs measured more than 70% which is a good correlation and the significance level came 0.000 for both analyses. For two vegetation indices WDRVI estimated 74% of correlation, which was higher than NDVI – FAPAR correlation (71%). Those regressions can be applicable to analyze

GPP or carbon uptake by the law of Monteith (1972).

When the seasonality analyzed for four study sites, it showed different index values, for example – length of season from NDVI time-series was 208 days in average but from WDRVI it was 128 days in average. Seasonal amplitude and small integral were also measured lower in case of WDRVI than NDVI. For all the parameters there were slight decreasing trend from 2001 to 2009 time-series.

Image analysis from TIMESAT showed more dynamic pattern of phenology of crops for south west of Skåne. Images on length of season showed contrast in 2005 from NDVI time-series but in WDRVI time-series it was not that much distinct for 2005. The spatial differences of length of season are more distinct in NDVI time-series rather than WDRVI time-series.

In case of amplitude and small integral from image analysis, it showed more distinct spatial pattern in NDVI than WDRVI index, contrast of the parameter were higher in NDVI than WDRVI images. But when NDVI images missed some pixels for small integral, WDRVI images estimated those areas with parameter values (figure 23 and 24 in year 2004 and 2006). So from results of image analysis, it was clear that coastal part of south west Skåne had less phenological variation for crop and the areas beside inland lakes and forest had more effect on crop phenology.

The peak of the indexes was for only like 30 or 45 days in a whole year so the absorption of radiation remained maximum for a short time period. So the high carbon sequestrations take place only for that time period. But it was not that much affective as the forest in summer because the crops are cut down after mature stage but the leaves remain grow in forest before winter. After the first season the residuals are kept on the field so for certain period there are emissions of carbon compounds from agricultural fields. It was observed in the time-series that most of the year there were the second season so the fields were almost covered by the green products for whole year and the agricultural lands are not allowed to keep bare in Sweden (to prevent soil erosion). After the primary season on summer the farmers start to seed another crop which lay under snow during winter and on that time the values of VIs show the lowest value in the time-series.

5.2. Possible errors from project

❖ Errors from field observation- The pixel of the MODIS images were 250m and the transects were taken 100m from only one edge of the crop field for all the study sites. So the PPF values could be vary little if all the parts of the field were observed in the study, so the reflectance of the rest of the part were not directly measured from the field or neglected for measure of FAPAR from fields. Cloudy days were missed for FAPAR observation, so the

data were not possible to taken in regular interval.

- ❖ Error from TIMESAT- TIMESAT could not cover dual seasons in some cases of the time-series, so the information on length of season and small integral might be presented in less parameter value in image analysis.

6. Conclusion

6.1. Conclusion on project result

Vegetation indexes are used to measure the green foliage density and to validate this measurement field data from TRAC were quite successful because the relationships were strong from equation 8 and 9, and both indices represent more than 70% of FAPAR. It is also possible to relate those equations into GPP from previous studies e.g. Gitelson *et al.* 2008.

All study sites were covered by green product except winter, so there was absorption of radiation for almost 9 months for all the years. So the production of carbon took places in the study sites. When the production scenario was analyzed through the images there was some dissimilarity between the results of different VIs. To get the exact phenology on crop, more than one indices value analysis is necessary.

TIMESAT is applicable in countries those have only one season or 2 seasons at most, but in tropical region people generally cultivate their agricultural land thrice a year which will be a difficult task for TIMESAT to cover all the seasons to get correct phenology. So it will be difficult to measure GPP from MODIS data through TIMESAT in tropical region especially for crops.

6.2. Further studies

- ❖ The relationship of FAPAR and MODIS derived VIs was found strong for crop, which are applicable to produce GPP estimation.
- ❖ It is possible to compare field FAPAR data with GPP data from tower flux data. That kind of comparison will give more realistic result on the relationship between GPP and FAPAR/ VIs.
- ❖ The application of TIMESAT on crops could be improved by considering all season's coverage for a year, so the project made the scope of improvement of TIMESAT software.
- ❖ Spatial pattern of crop distribution and phenology can be analyzed for not only in Skåne but also for whole Sweden.
- ❖ Food production can be estimated by satellite remote sensing. When we have the NDVI or WDRVI values, we can measure the GPP of a region or pixel.
- ❖ Climate change and its impact on crop can be analyzed from the comparison on changes of

climatic variables and crop phenology. For example, we can make regression on temperature and GPP of area which will show the impacts of regional climate on food production.

- ❖ Food productivity can be forecast with the future climate conditions from different models. So countries with food scarcity can take proper action and future plan to ensure food security for their people.

References

- Asrar, G., Fuchs, M., Kanemasu, E. T., Hatfield J. H., 1984. Estimating absorbed photosynthetic radiation and leaf area index from spectral reflectance in wheat. *Agron.J.*, vol. 76, pp. 300-306.
- Chen, J., 1996. Evaluation of vegetation indices and a modified simple ratio for boreal applications. *Canadian Journal of Remote Sensing*, 22, 229-242.
- Colwell, R. N. (Ed.), 1983. *Manual of Remote Sensing*, 2nd. Ed., Falls Church, VA: American Society of Photogrammetry.
- Bärring L, Jönsson P., Mattsson J. O., Åhman R, 2003. Wind erosion on arable land in Scania, Sweden and relation to the wind climate- a review. *Catena* 52, 173-190.
- Berglund, B.E., Larsson, L., Lewan, N., Skasjö, S., Riddersporre, M. (Eds.), 1991. The Cultural Landscape During 6000 Years in Southern Sweden: The Ystad Project. *Ecological Bulletins*, vol. 41. Munksgaard, Copenhagen. 495 pp.
- Blennow, K., Bärring, L., Jönsson, P., Linderson, M. L., Mattsson, J.O., Schlyter, P., 1999. Klimat, sjöar och vattendrag. In: Germundsson, T., Schlyter, P. (Eds.), *Atlas över Skåne*. Sveriges Nationalatlas, Stockholm, pp. 30-37.
- EEA, 2010. <http://www.eea.europa.eu/data-and-maps/data/corine-land-cover-clc1990-250-m-version-12-2009> (Accessed on 20-3-2010)
- Eklundh, L. and Jönsson, P., 2003, Extracting Information about Vegetation Seasons in Africa from Pathfinder AVHRR NDVI Imagery using Temporal Filtering and Least-Squares Fits to Asymmetric Gaussian Functions. In *Image and Signal Processing for Remote Sensing VIII. Proceedings of SPIE Vol 4885*, edited by Serpico. S.S. Society of Photo-Optical Instrumentation Engineers, pp. 215-225.
- Gitelson, A. A., 2004. Wide dynamic range vegetation index for remote quantification of biophysical characteristics of vegetation. *Journal of Plant Physiology* 161, 165-173.
- Gitelson, A. A., Viña, A., Masek, J. G., Verma, S. B., Suyker, A. E., 2008. Synoptic Monitoring of Gross Primary Productivity of Maize Using Landsat Data. *IEEE Geoscience and Remote Sensing Letters*, Vol. 5, No. 2, 133-137.
- Glenn, E. P., Huete A. R., Naglar, P. L., Nelson, S. G., 2008. Relationship between

Remotely-sensed Vegetation Indices, Canopy Attributes and Plant Physiological Processes: What Vegetation Indices Can and Cannot Tell Us About the Landscape. *Sensors*, 8, 2136-2160.

Goward, S.N., Dye, D.G., 1987. Evaluating North American net primary productivity with satellite observations. *Advances in Space Research*, Vol. 7, 165–174.

Goward, S. N. & Huemmrich, K. F., 1992. Vegetation canopy PAR absorptance and the normalized difference vegetation index: An assessment using the SAIL model. *Remote Sensing of the Environment*, vol.39, 2, pp. 119-140.

Goward, S., Waring, R., Dye, D., & Yang, J., 1994. Ecological remote sensing at otter: Satellite macroscale observations. *Ecological Applications*, 4, 322-343.

Henebry, G.M., Viña A., Gitelson A. A., 2004. The Wide Dynamic Range Vegetation Index and its Potential Utility for Gap Analysis. Center for Advanced Land Management Information Technologies(CALMIT), *Gap Analysis Bulletin* No.12 50-56. <http://www.gap.uidaho.edu/bulletins/12/The%20Wide%20Dynamic%20Range%20Vegetation%20Index.htm> (Accessed on 20-7-2010).

Huete, A. and Justice, C., 1999. *MODIS Vegetation Index (MOD 13) Algorithm Theoretical Basis document*, Greenbelt: NASA Goddard Space Flight Center, <http://modarch.gsfc.nasa.gov/MODIS/LAND/#vegetation-indices>, 129pp.

Jensen, J. R., 2000. *Remote Sensing of the Environment- An earth resource perspective*. Prentice Hall, Upper Saddle River, New Jersey 07458.

Jönsson, P. and Eklundh, L., 2002, Seasonality extraction by function fitting to time-series of satellite sensor data, *IEEE Transactions on Geoscience and Remote Sensing*, 40, 1824-1832.

Jönsson, P. and Eklundh, L., 2003. Seasonality extraction from satellite sensor data. In *Frontiers of Remote Sensing Information Processing*, edited by Chen, C.H. World Scientific Publishing. pp 487-500.

Jönsson, P. and Eklundh, L., 2004. TIMESAT - a program for analysing time-series of satellite sensor data, *Computers and Geosciences* 30, 833-845.

Larcher, W., 2003. *Physiological plant ecology- Ecophysiology and stress physiology of functional groups*, (4th ed.). Berlin Springer-Verlag.

Mattsson, J.O., 1987. Vinderosion och klimatändringar. Kommentarer till 1700-talets

ekologiska kris i Skåne (English summary: Wind erosion and climatic changes. Comments on the ecological crisis of Skåne during the 18th century). *Sw. Geogr. Yearb.* 63, 94-108.

MODLAND. *MODLAND Tile calculator*. October 12, 2005. <http://modis-250m.nascom.nasa.gov/cgi-bin/developer/tilemap.cgi> (accessed July 20, 2010).

Monteith, J. L., 1972. Solar radiation and productivity in tropical ecosystems. *J. Appl. Ecol.*, Vol.9, no. 3, 744-766.

NASA 1, 2010. <http://www.csc.noaa.gov/products/sccoasts/html/rsdetail.htm> (Accessed on 10-5-2010).

Olofsson, P. & Eklundh, L., 2007. Estimation of absorbed PAR across Scandinavia from satellite measurements. Part II: Modeling and evaluating the fractional absorption. *Remote Sensing of Environment* 110, 240-251.

Rous, J.W., Haas R.H., Schell J.A. and Deering D.W., 1974, "Monitoring vegetation Systems in the great plains with ERTS," *Proceedings*, Third Earth Resources technology Satellite-1 Symposium, Greenbelt: NASA SP-351, 3010-317.

Ruimy, A., Saugier, B., Dedieu, G., 1994. Methodology for the estimation of terrestrial net primary production from remotely sensed data. *Journal of Geophysical Research* 99, 5263–5283.

Running, S.W., Nemani, R.R., 1988. Relating seasonal patterns of the AVHRR vegetation index to simulated photosynthesis and transpiration of forests in different climates. *Remote Sensing of Environment* 24, 347–367.

Running, S.W., C.O. Justice, V.Solomonson, D. Hall, J. Barker, Y.J. Kaufmann, A.H.Strahlar, A.R. Huete, J.P.Muller, V.Vanderbilt, Z.M. Wan, P. Teillet and D.Carnrggie, 1994, "Terrestrial Remote Sensing Science and algorithms Planned for EOS/MODIS", *Intl. Journal of Remote Sensing*, 15(17):3587-3620.

SACCESS. <http://saccess.lantmateriet.se/order/simpleverify> (Accessed on 21-05-2010)

Schubert, P.,Eklundh L., Lund M., Nilsson M., 2010. Estimating northern peatland CO2 exchange from MODIS time series data, *Remote Sensing of Environment*, doi: 10.1016/j.rse.2010.01.005

Van Leeuwen, W., & Huete, A., 1996. Effects of standing litter on the biophysical interpretation of plants canopies with spectral indices. *Remote Sensing of Environment*, 55, 123-138.

Viña, A., Henebry G. M., and Gitelson A. A., 2004. Satellite monitoring of vegetation dynamics: Sensitivity enhancement by the Wide Dynamic Range Vegetation Index. *Geophysical Research Letters* . Vol. 31 (4)L04503. Doi:10.1029/2003GL19034.

Viña, A. and Gitelson A. A., 2005. New developments in the remote estimation of the fraction of absorbed photosynthetically active radiation in crops. *Geophysical Research Letters*, vol. 32, no. 17, p. L17 403, DOI: 10.1029/2005GL023647.

Xiao, X.; Zhang, Q.; Braswell, B.; Urbanski, S.; Boles, I.; Wofsy, S.; Moore, B.; Ojima, D., 2004. Modeling gross primary production of temperate deciduous broadleaf forest using satellite images and climate data. *Remote Sensing of Environment*, 91, 256-270.

Appendix A

Abbreviations used in report:

Ag = Green area on each plot/site.

APAR= Photosynthetically active radiation absorbed by vegetation

AVHRR = Advanced Very High Resolution Radiometer

ϵ =vegetation capacity to convert radiation energy to biomass.

FAPAR = Fraction of absorbed photosynthetically active radiation

FIPAR = Fraction of intercepted photosynthetically active radiation

GPP = Gross primary productivity, Total CO₂ assimilation through photosynthesis

GUI = Graphical user interface

LAI = Leaf Area Index

MODIS = Moderate Resolution Imaging Spectroradiometer

NDVI = Normalized difference vegetation index

NE Δ GPP = Noise equivalent of GPP

NPP = Net primary production

PPFD_I = Incoming photosynthetic photon flux density

PPFD_R = Reflected photosynthetic photon flux density.

VI = Vegetation index

WDRVI = Wide Dynamic Range Vegetation Index

Publication list:

The reports are available at the Geo-Library, Department of Physical Geography, University of Lund, Sölvegatan 12, S-223 62 Lund, Sweden.

Report series started 1985. The whole complete list and electronic versions are available at <http://www.geobib.lu.se/>

- 156 Cederlund, Emma (2009): Metodgranskning av Klimatkommunernas lathund för inventering av växthusgasutsläpp från en kommun
- 157 Öberg, Hanna (2009): GIS-användning i katastrofdrabbade utvecklingsländer
- 158 Marion Früchtl & Miriam Hurkuck (2009): Reproduction of methane emissions from terrestrial plants under aerobic conditions
- 159 Florian Sallaba (2009): Potential of a Post-Classification Change Detection Analysis to Identify Land Use and Land Cover Changes. A Case Study in Northern Greece
- 160 Sara Odelius (2009): Analys av stadsluftens kvalitet med hjälp av geografiska informationssystem.
- 161 Carl Bergman (2009): En undersökning av samband mellan förändringar i fenologi och temperatur 1982-2005 med hjälp av GIMMS datasetet och klimatdata från SMHI.
- 162 Per Ola Olsson (2009): Digitala höjdmodeller och höjdsystem. Insamling av höjddata med fokus på flygburen laserskanning.
- 163 Johanna Engström (2009): Landskapets påverkan på vinden -sett ur ett vindkraftperspektiv.

- 164 Andrea Johansson (2009): Olika våtmarkstypers påverkan på CH₄, N₂O och CO₂ utsläpp, och upptag av N₂.
- 165 Linn Elmlund (2009): The Threat of Climate Change to Coral Reefs
- 166 Hanna Forssman (2009): Avsmältningen av isen på Arktis - mätmetoder, orsaker och effekter.
- 167 Julia Olsson (2009): Alpina trädgränsens förändring i Jämtlands- och Dalarnas län över 100 år.
- 168 Helen Thorstensson (2009): Relating soil properties to biomass consumption and land management in semiarid Sudan – A Minor Field Study in North Kordofan
- 169 Nina Cerić och Sanna Elgh Dalgren (2009): Kustöversvämningar och GIS
- en studie om Skånska kustnära kommuners arbete samt interpolations-metodens betydelse av höjddata vid översvämningssimulering.
- 170 Mats Carlsson (2009): Aerosolers påverkan på klimatet.
- 171 Elise Palm (2009): Övervakning av gåsbete av vass – en metodutveckling
- 172 Sophie Rychlik (2009): Relating interannual variability of atmospheric CH₄ growth rate to large-scale CH₄ emissions from northern wetlands
- 173 Per-Olof Seiron and Hanna Friman (2009): The Effects of Climate Induced Sea Level Rise on the Coastal Areas in the Hambantota District, Sri Lanka - A geographical study of Hambantota and an identification of vulnerable ecosystems and land use along the coast.
- 174 Norbert Pirk (2009): Methane Emission Peaks from Permafrost Environments: Using Ultra-Wideband Spectroscopy, Sub-Surface Pressure Sensing and Finite Element Solving as Means of their Exploration
- 175 Hongxiao Jin (2010): Drivers of Global Wildfires — Statistical analyses
- 176 Emma Cederlund (2010): Dalby Söderskog – Den historiska utvecklingen
- 177 Lina Glad (2010): En förändringsstudie av Ivösjöns strandlinje
- 178 Erika Filppa (2010): Utsläpp till luft från ballastproduktionen år 2008
- 179 Karolina Jacobsson (2010): Havsisens avsmältning i Arktis och dess effekter
- 180 Mattias Spångmyr (2010): Global of effects of albedo change due to urbanization

- 181 Emmelie Johansson & Towe Andersson (2010): Ekologiskt jordbruk - ett sätt att minska övergödningen och bevara den biologiska mångfalden?
- 182 Åsa Cornander (2010): Stigande havsnivåer och dess effect på känsligt belägna bosättningar
- 183 Linda Adamsson (2010): Landskapsekologisk undersökning av ädellövskogen i Östra Vätterbranterna
- 184 Ylva Persson (2010): Markfuktighetens påverkan på granens tillväxt i Guvarp
- 185 Boel Hedgren (2010): Den arktiska permafrostens degradering och metangasutsläpp
- 186 Joakim Lindblad & Johan Lindenbaum (2010): GIS-baserad kartläggning av sambandet mellan pesticidförekomster i grundvatten och markegenskaper
- 187 Oscar Dagerskog (2010): Baösbergsgrottan – Historiska tillbakablickar och en lokalklimatologisk undersökning
- 188 Mikael Månsson (2010): Webbaserad GIS-klient för hantering av geologisk information
- 189 Lina Eklund (2010): Accessibility to health services in the West Bank, occupied Palestinian Territory.
- 190 Edvin Eriksson (2010): Kvalitet och osäkerhet i geografisk analys - En studie om kvalitetsaspekter med fokus på osäkerhetsanalys av rumsrig prognosmodell för trafikolyckor
- 191 Elsa Tessaire (2010): Impacts of stressful weather events on forest ecosystems in south Sweden.
- 192 Xuejing Lei (2010): Assessment of Climate Change Impacts on Cork Oak in Western Mediterranean Regions: A Comparative Analysis of Extreme Indices
- 193 Radoslaw Guzinski (2010) Comparison of vegetation indices to determine their accuracy in predicting spring phenology of Swedish ecosystems